UNITED NATIONS EDUCATIONAL, SCIENTIFIC AND CULTURAL ORGANIZATION
INTERNATIONAL ATOMIC ENERGY AGENCY
INTERNATIONAL CENTRE FOR THEORETICAL PHYSICS
I.C.T.P., P.O. BOX 586, 34100 TRIESTE, ITALY, CABLE: CENTRATOM TRIESTE

H4.SMR/984-14

Winter College on Quantum Optics: Novel Radiation Sources

3-21 March 1997

Soft X-ray laser applications

J. Rocca

**Department of Electrical Engineering, Colorado State University,
Fort Collins, USA**

INTRODUCTION TO ULTRASHORT WAVELENGTH LASERS
X-RAY LASERS: FUNDAMENTALS AND DEVICES

Jorge J. Rocca
Electrical Engineering Department
Colorado State University
Fort. Collins, CO 80523
February 1997

INTRODUCTION

Shortly after the demonstration of the first lasers in 1960, it was realized that the concept could be extended to the x-ray region of the spectrum. It was also recognized that the development of x-ray lasers would be a very challenging task. In fact, it was not until 1984 that the first demonstration of large amplification in the soft x-ray region was achieved [1,2], utilizing as energy source for such devices very powerful lasers. During the decade that followed most of the x-ray laser research and development, with only a several exceptions, has been conducted at laboratories equipped with very energetic laser sources, of the type utilized in inertial confinement nuclear fusion research. Only recently large amplification has been demonstrated utilizing more compact, or "table top" size drivers.

In great part the difficulties are associated with the very large power density deposition required for the creation of an x-ray laser amplification medium with the necessary large population inversions. Such a requirement is exacerbated by the difficulty of utilizing optical resonators due to the poor reflectivity of materials at normal incidence, and to the usually short lifetime of the gain.

In the absence of multiple pass amplification (double pass amplification has been demonstrated in several experiments and triple pass amplification in at least one case, (see Section 3) a large gain is required to produce an intense beam by amplification of the spontaneous emission in a single pass through the amplifier. Normally an amplification of at least exp (5), corresponding to a gain-length product of 5 is necessary to clearly amplify the laser line to an intensity well above that of other strong spontaneous emission lines in the same medium. To efficiently extract the energy stored in the population inversion by saturating the gain a significantly larger gain-length is required, approximately gl ï 15 in collisionally pumped amplifiers, the only ones in which gain saturation has been achieved to date.

The next section reviews the concept of amplification of radiation in a homogeneous column, including the expressions for the gain and the intensity increase as a function of plasma length in a non-saturated medium. These topics and several of the concepts discussed in these notes are covered in the book by R. C. Elton [3], which also constitutes a good review of the status of the field of x-ray lasers up to 1990. These notes are limited to the discussion of the generation of coherent ultrashort wavelength radiation by

amplified spontaneous emission in plasmas. Other ways to produce such radiation, as harmonics generation (an important option for applications in which low peak intensities and high repetition rate is required) and free electron lasers are not included in our review.

GAIN AND INTENSITY AMPLIFICATION

As in any other type of laser amplifier, in a homogeneous x-ray laser amplifier column the variation of the intensity of an injected beam with plasma length depends on the intensity increase caused by stimulated emission and the attenuation caused by absorption. Neglecting of other types of losses, such as that caused by refraction, the variation of the x-ray beam as a function of length can be computed from:

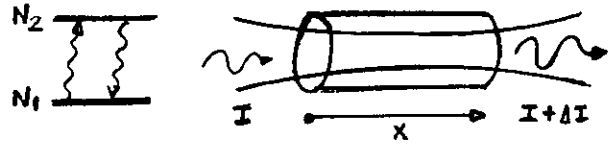

Figure 1 - Amplification of an injected beam in a homogeneous laser amplifier.

$$\frac{dI}{dx} = \underbrace{N_2 B_{21} \frac{I}{c} h\nu\, g(\nu)}_{\text{STIMULATED EMISSION}} - \underbrace{N_1 B_{12} \frac{I}{c} h\nu\, g(\nu)}_{\text{ABSORPTION}} \qquad (1)$$

where N_2 and N_1 are the laser upper and lower level density and g(v) is the lineshape function.

Substituting the Einstein B_{12} and B_{21} coefficients as a function of the A_{21} spontaneous emission coefficient:

$$B_{21} = \frac{g_1}{g_2} B_{12} \;,\; \frac{A_{21}}{B_{21}} = \frac{8\pi h\nu^3}{c^3} \qquad \text{and using } \nu = \frac{c}{\lambda}$$

$$\frac{dI}{dx} = \left[A_{21} \frac{\lambda^2}{8\pi} g(\nu) \left(N_2 - N_1 \frac{g_2}{g_1} \right) \right] = \sigma(\nu) \Delta N\, Iv = g_o(\nu)\, I_\nu \qquad (2)$$

Integrating $$I_\nu(z) = I_\nu(o)\, e^{g_o x} \qquad (3)$$

where the small signal gain coefficient g_o can be written as the product of the stimulated emission cross section $$\sigma(\nu) = \frac{A_{21}}{8\pi}\lambda^2\, g(\nu) \qquad (4)$$

and the population inversion density

$$\Delta N = \left(N_2 - N_1 \frac{g_2}{g_1}\right) \qquad (5)$$

$$g(\nu) = \sigma(\nu)\,\Delta N \qquad (6)$$

The stimulated emission cross section determines the inversion necessary to obtain a required gain (for example $1cm^{-1}$).

For example for the λ = 182Å Balmer Alpha line of Hydrogen-like Carbon (n=3 to n=2 line) which has been demonstrated to amplify following plasma recombination [2], the stimulated emission cross section at line center is, as computed below,
$\sigma \approx 4.4\,10^{15} cm^2$, requiring an inversion of $\Delta N = 2.310^{14} cm^{-3}$ for a gain coefficient of $1cm^{-1}$.

Assuming a Doppler broadened line for an ion temperature at the time of lasing of T_i = 20eV,

$$g(\nu_o) = \left(\frac{4\ln 2}{\pi}\right)^{1/2} \frac{1}{\Delta\nu_D} = \frac{0.94}{\Delta\nu_D} \approx \frac{1}{\Delta\nu_D}$$

with $$\frac{\Delta\nu_D}{\nu} = 7.7\,10^{-5}\sqrt{\frac{k_B T}{M}} \quad (M_{Te}\ in\ ev,\ M\ in\ AMU)$$

For $\begin{matrix} k_B T_i = 20\,ev \\ M = 12\,AMU \end{matrix} \Rightarrow \frac{\Delta\nu_D}{\nu} = 1 \times 10^{-4} \rightarrow \Delta\nu = 10^{-4}\,\nu_o$

$$A_{21} = 6.6\,10^{15}\left(\frac{g_1}{g_2}\right)\frac{F_{12}}{\left[\lambda\left(\overset{o}{A}\right)\right]^2} = 5.66\,10^{10}\ s^{-1}$$

$$\sigma = \frac{5.7\,10^{10}}{8\pi}\,\frac{\lambda^3}{c\left(\frac{\Delta\nu}{\nu}\right)} = \frac{5.7\,10^{10}}{8\pi}\,\frac{\left(180\,10^{-8}\right)^3}{1 \times 10^{-4}\ 3 \times 10^{10}} = 4.4\,10^{-15} cm^2$$

Nevertheless in an x-ray the beam is usually not injected, but it grows from the spontaneous emission. Designating by the spontaneous emission by unit length:

$$\frac{dI}{dx} = J\, e^{gx} \qquad (7)$$

$$I = \frac{Js}{g}\left(e^{g\ell} - 1\right) \qquad (8)$$

The above expression, in which for maximum gain g is the gain at line center, is not accurate to analyze the result of experiments because in most cases the detection instruments do not spectrally resolve the line profile and consequently provide a measurement of the spectrally integrated intensity. Therefore, to obtain an expression of the length dependence of the x-ray laser beam power P that is useful for the experimentalists, it is necessary to integrate in frequency over the time profile. Such a result was first obtained by Lindford [4] (who was analyzing higher gain infrared lasers).

Integrating over length, angle and frequency

$$P = \int_0^\infty \int_0^\ell \int_{d\Omega} h\nu\, A_{21}\, N\, g(\nu)\, \frac{e^{g\ell - 1}}{g}\, \frac{d\Omega}{4\pi}\, d\nu\, d\nu \qquad (9)$$

A Taylor series expansion can be used to integrate since the lineshape function is sharply peaked about the center frequency, resulting in:

$$P = \frac{A\Omega}{4\pi}\left[h\nu^3\,\frac{8\pi}{c^2}\left(\frac{\pi\, g(o)}{2\, g''(o)}\right)^{1/2}\right]\ \frac{\left[e^{g(o)\ell} - 1\right]^{1/2}}{\left[e^{g(o)\ell}\right]^{1/2}\left(go\ell\right)^{1/2}} \qquad (11)$$

where g(o) and g"(o) are the value and second derivative of the lineshape function at line center ($\nu = \nu_o$). The results are valid for any sharply peaked line profile symmetric about ν_o and is therefore valid for both a gaussian (Doppler broadened) or Lorentzian line profile.

This equation gives the 3/2 over 1/2 dependence of the power:

$$P \;\alpha\; \frac{\left[e^{g(o)\ell}-1\right]^{3/2}}{\left[g(o)\ell e^{g(o)\ell}\right]^{1/2}} \qquad (12)$$

which is most commonly used to fit experimental data of laser power as a function of plasma column length to determine the gain. It is accurate for all values of g(o)l, as shown in figure 2 in comparison with an exact solution to the radiation propagation equation computed numerically.

The Lindford derivation assumes a gain medium without inhomogeneites and does not take into account depletion of the population inversion by the laser beam which ultimately saturates the increase of the laser power as a function of length.

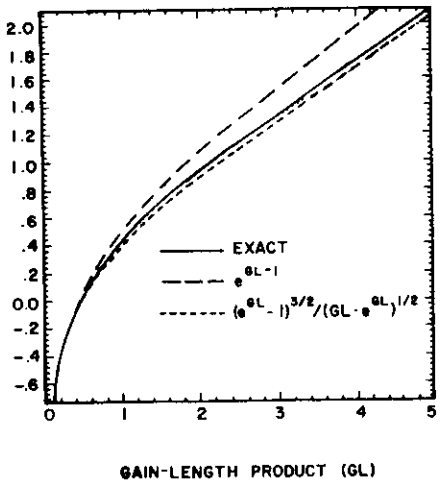

Figure 2 - Exact solution of the radiation transport equation in an homogeneous amplifier, as compared with the Linford formula and the $(e^{g}-1)$ approximations. After ref. [3]., from a calculation by R. London.

GAIN AND POWER SATURATION

In integrating expression (1) we considered the populations to be independent of the laser intensity. However, for large $g_o \ell$ the laser intensity is sufficiently intense to deplete the population inversion and limit the exponential growth of the laser power. The intensity at which the population inversion and consequently the gain are reduced by half is defined as the saturation intensity, and can be approximately calculated by [5]:

$$I_s = \frac{h\nu}{\sigma(\nu_o)\,\tau_2} \qquad (13)$$

for the case in which the upper level lifetime $\tau_2 >> \tau_1$, where τ_1 is the lower level lifetime (a quite common case). For the inhomogeneously broadened (Doppler broadened) line it can be shown that the gain decreases as a function of intensity as [5]:

$$g(\nu, I) = \frac{\Delta N\,\sigma(\nu)}{\left(1+\frac{I_\nu}{I_s}\right)^{1/2}} = \frac{g_o(\nu)}{\left(1+\frac{I_\nu}{I_s}\right)^{1/2}} \qquad (14)$$

where $g_o(\nu)$ is the gain at small intensities or small signal gain.

In computing the saturation intensity, it is important to consider that collisional processes might shorten the upper level lifetime, τ_2, significantly below the $\tau_{21} = \left[A_{21}\right]^{-1}$ value.

For example, for the λ = 46.9 nm, J = 0 -1 line of Neon-like Argon, a line recently demonstrated to lase in both discharge and laser pumped mediums [7,8], electron collisions from the 3p upper laser level of the 3d levels shorten the lifetime of the 3p level by a factor 10-30, depending on the plasma conditions.

Considering $A_{21} \approx 1 \times 10^{10}$

$$\frac{\tau_{21}}{\tau_2} = \frac{1}{A_{21}\,\tau_2} = 20$$

and a Doppler broadened profile for an ion temperature of T_i=100eV

$\sigma(\nu_o) \approx 1.1\,10^{-14} cm^2$, and neglecting τ_1

The saturation intensity is computed to be $I_s \approx 77 MW/cm^2$. Further consideration that in this case the lower level lifetime τ_1 is not negligible as compared to the effective lifetime of the upper level moderately reduces this value.

Only a few soft x-ray laser systems have achieved to date sufficiently large gain-length products to saturate the gain [9-11]. The results of experiments showing gain saturation in the collisionally excited line of Ne-like Se and Ne-like Ge are shown in figure 3.

The above results are typical of collisionally excited laser lines in Ne-like ions where saturation has been observed for gl ~ 14 - 18 [9-11].

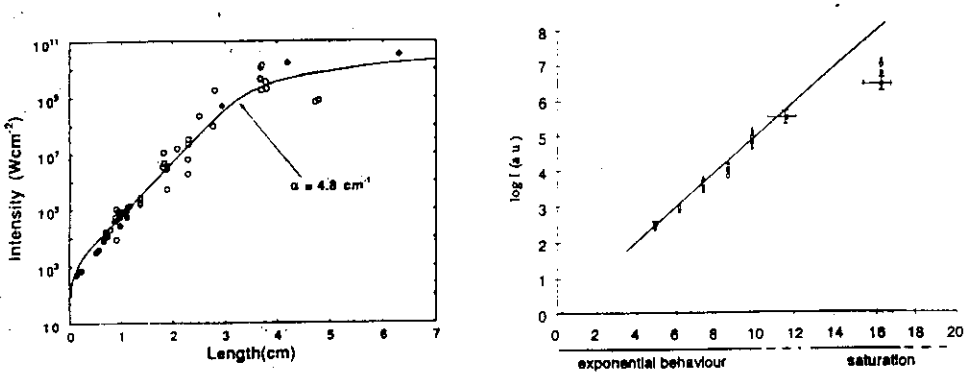

Figure 3 - a) Scaling of the intensity of a Ne-like Selenium 206.4Å soft x-ray amplifier , and b) of 212 Å Ne-like Zinc laser as a function of plasma length, from reference 9 and 10 respectively. The above results are typical of collisional excited laser transitions in Ne-like ions where gain saturation has been observed for gl = 14-18 .

PUMP POWER REQUIREMENTS

The pumping power required to pump a selected x-ray laser transition depends on the particular transition and lasing scheme. However, an estimate of the minimum pumping power required can be obtained calculating the power necessary to compensate the spontaneous emission power radiated by the laser upper level population [3], as shown below.

The power radiated per unit volume by a level with population density N_2 is

$$\frac{P}{V} = N_2 \, A_{21} \, h\nu_{21} \tag{10}$$

where

$$g_o = \sigma \, \Delta N \sim \sigma \, N_2 \rightarrow N_2 = \frac{g_o}{\sigma}$$

substituting the stimulated emission cross section for (4), and using

$$\frac{\Delta \nu}{\nu} = \frac{\Delta \lambda}{\lambda} \Rightarrow \Delta \nu = \frac{\Delta \lambda c}{\lambda^2}$$

$$P(h\nu) = 8\pi \frac{g_o \ell}{\lambda^4} hc^2 \left(\frac{\Delta\lambda}{\lambda}\right) A \tag{15}$$

where the volume has been substituted as a function of plasma column length l and cross section A. But considering typically that only a small fraction F of the pump power is deposited in the laser upper level and that the quantum efficiency of the laser $q_E < 1$, the minimum pump power required is:

$$P = \frac{1}{F q_E} 8\pi \frac{g_o \ell}{\lambda^4} hc^3 \left(\frac{\Delta\lambda}{\lambda}\right) A \tag{16}$$

If we require it to be sufficiently large as to saturate the transition, gl = 15, and if we assume $\frac{\Delta\lambda}{\lambda} = 10^{-4}$ (a typical value of the relative linewidth) for a plasma column 100μm in radius we obtain for λ = 100 Å and λ = 10 Å respectively:

P_{PUMP} (λ = 100 Å) = 3 x 10^{10} W

P_{PUMP} (λ = 10 Å) = 3 x 10^{14} W

where we assumed F = 0.01 and q_E = 0.1 For the shorter wavelength (10 Å), where x-ray lasers have not yet been demonstrated, both practical and fundamental limitations, will

require the use of very small diameter columns. It is clear that very large power drivers are necessary. To achieve the necessary power density deposition successful experiments to date have utilized as drivers the same kind of very large laser utilized in inertial fusion research [1,9,13], and more recently, powerful picosecond and subpicosecond lasers [14,15], and fast electrical discharges [7,16].

SCALING OF THE GAIN WITH PLASMA DENSITY

PLASMA DENSITY REQUIREMENTS

Simple considerations show that to obtain large amplification of soft x-ray transitions from multiple ionized ions (Z ≥ 10) requires amplifying columns with large plasma density.

For a gain length product sufficient to achieve gain saturation, we require

$$G\ell > N_2\,\sigma\ell\,F_{inv} \geq 15 \qquad (16)$$

where here F_{inv} is the "inversion factor" that takes into account the fact that the upper laser level population density is larger than the population inversion density.

$$F_{inv} = 1 - \frac{N_1}{N_2}\frac{g_2}{g_1} < 1$$

Substituting the stimulated emission cross section by (4) with $\frac{\Delta\lambda}{\lambda} \approx 10^{-4}$, and assuming $F_{inv} \approx 0.3$, and an absorption oscillator strength $f_{01} = 0.5$

$$N_2\left(cm^{-3}\right)\ell \geq \frac{15}{0.3\sigma} \approx \frac{15}{0.3\left[6.6\,10^{-15}\,\frac{g_1}{g_2}\,\frac{f_{12}}{\lambda^2}\right]\frac{\lambda^2}{8\pi}\,\frac{1}{\Delta\nu}}$$

with $$\sigma = 6.6\,10^{15}\,\frac{g_1}{g_2}\,\frac{f_{12}}{\lambda^2\left(\overset{o}{A}\right)}\,\frac{\lambda^2\left(\overset{o}{A}\right)10^{-6}}{8\pi\,\Delta\nu}$$

and $$\Delta\nu = \frac{\Delta\lambda}{\lambda}\,\frac{\lambda}{c} \approx 3\,10^{-4}\,\frac{\lambda}{c}$$

for $f_{12} = 0.5$, $g_1/g_2 = 3/5$ (case of $J = 2$-1 lines in Ne-like ions) results:

$$N_e\ell\left(\frac{1}{cm^2}\right) = \frac{6\,10^{18}}{\lambda\left(\overset{o}{A}\right)}$$

considering that the density of laser upper ions to ground state ions is $N_2/N_o = 3\text{x}10^{-3}$ [Elton], that the relative abundance of that ion is 30%, $N_o/N_T = 0.3$ and assuming that the ions are 20 times ionized (Z=20)

$$N_e = ZN_i \qquad N_e\,\ell = N_2\ell\,\frac{N_o}{N_2}\,\frac{N_T}{N_o}\,Z$$

$$N_e\,\ell \approx \frac{3\,20}{3\,10^{-3}}\;\frac{6\,10^{18}}{\lambda\left(\overset{o}{A}\right)} = \frac{1.2\,10^{23}}{\lambda\,(A)}\;\frac{1}{cm^2} \qquad (17)$$

that for a λ =100 Å laser in a 5cm long plasma is

$$N_e\left(\lambda = 100\right) \approx 2.4\,10^{20}\;cm^{-3}$$

which is an enormous density when compared with that of a visible Argon ion laser ($Ne < 10^{14}cm^{-3}$).

From equation (16) and the proportionality of the upper level population with electron density, it results that gl increases with N_e, however, there are several processes besides pump power limitations that limit the maximum electron density for a given laser system and that define an optimum electron density. These effects are summarized below and are also discussed in Elton's book [3].

LIMITATIONS OF THE MAXIMUM PLASMA DENSITY

QUENCHING OF THE POPULATION INVERSION BY ELECTRON COLLISIONS

Let us consider the simplified energy level diagram of figure 4, typical of some practical laser systems, in which the laser upper level is excited at a rate N_eR_{o2}, and de-excited both radiatively and by electron collisions to the laser lower level 1.

The population inversion can be computed from the following equations,

$$\frac{dN_2}{dt} = N_0\ R_{02}\ N_e - N_2\left(A_{21} + N_e\ R_{d21}\right)$$

$$\frac{dN_1}{dt} = N_2\ \left(A_{21} + N_e\ R_{d21}\right) - N_1\ A_{10} \qquad (18)$$

where R_{d21} is the rate constant for de-excitation from the upper to the lower laser upper level. In steady state, the population inversion results (for $g_2/g_1 = 1$):

$$N_2 - N_1\frac{g_2}{g_1} = N_2\left[1-\left(\frac{A_{21}+N_e\ R_{d21}}{A_{10}}\right)\right] =$$

$$= \frac{N_0\ R_{02}\ N_e}{\left(A_{21}+N_e\ R_{d21}\right)}\left[1-\frac{A_{21}+N_e\ R_{d21}}{A_{10}}\right] \qquad (19)$$

Notice that when $N_e\ R_{d21} \sim A_{21}$ the increase of the population of the upper level starts to saturate. At even higher densities, the term in parenthesis destroys the population inversion and consequently the gain vanishes.

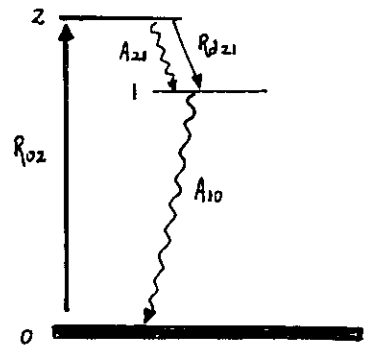

Figure 4 - Simplified energy level diagram of a soft x-ray laser amplifier

The optimum electron density can be estimated maximizing equation (19), with respect to Ne. As an example, the variation of the gain as a function of the N_eR_{d21}/A_{10} ratio is plotted in figure 5 for A_{10}/A_{21} as parameter. In the case $A_{10} = 10A_{21}$, the small signal gain is observed to reach a maximum when the electron de-excitation rate of the upper laser level is about 20% of its radiative decay rate.

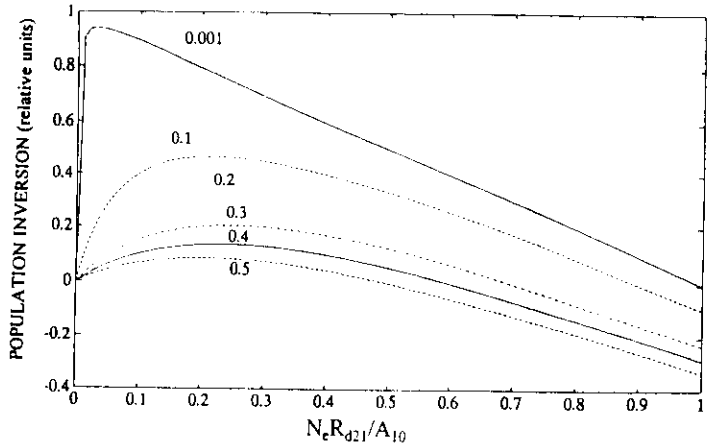

Figure 5 - Computed value of the population inversion as a function of N_eR_{d21}/A_{10} ratio with ratio of upper level to lower level lifetime as parameter.

To compare the optimum electron density we must calculate the de-excitation rate constant R_{21}, which can be computed from the rate of de-excitation R_{12} utilizing the principle of detailed balance.

Assuming equilibrium

$$R_{21} = <\sigma_{21}\ v>\ N_2 = <\sigma_{12}\ \sigma>\ N_1 = R_{10} \qquad (20)$$

and $$\frac{N_2}{N_1} = \frac{g_2}{g_1}\ e^{-\left(\frac{E_2-E_1}{k_B T_e}\right)}$$ (thermal equilibrium)

results in:

$$R_{21} = <\sigma_{12}\ V> = <\sigma_{12}\ V>\frac{g_1}{g_2}\ e^{\Delta E/k_B T_e} \qquad (21)$$

where $<\sigma V>$ represents the integral of the product of excitation (or de-excitation) cross section and the velocity averaged over a Maxwellian distribution.

In the case of an electric dipole transition, the electron-collisional excitation rate constant can be computed using the modified Coulomb-Born formula [3] by:

$$R_{12} = 1.6\,10^{-5}\ \frac{f_{12} < g_{12} >}{\Delta E_{12}\,(k_B T_e)^{1/2}}\ \exp\left(\frac{-\Delta E}{k_B T_e}\right)\frac{cm^3}{s} \qquad (22)$$

where $< g_{12} >$ is the effective Gaunt factor averaged over a Maxwellian distribution. For values of the electron energy $k_B T_e \leq \Delta E$ the effective Gaunt factor can be taken to be approximately 0.2 for many ions, at least when $N_2 - N_1 \geq 1$. For $\Delta\eta = 0$ (such as the 3p-3s laser transitions in Ne-like ions) the validity of the above formalism is questionable, but it has been suggested by Elton, that the above formula with an effective Gaunt factor $< g_{12} > \approx 1.5$ can be used as a first approximation [3].

REFRACTION

Another limit to the maximum usable plasma density is imposed by refraction effects, that bend the x-ray beam out of the gain volume, causing a loss (a decrease in the effective gain) and in extreme cases limiting the maximum amplification length. The effect of refraction is summarized below. The problem of refraction on x-ray amplifiers was early recognized by Chirkov [17] and later analyzed in detail by London [18]. The index of refraction in a plasma which is given by

$$\eta = \sqrt{1 - \left(\frac{n_e}{n_{ec}}\right)^2} \qquad (23)$$

where η_{ec} is the critical density,

$$\eta_{ec} = \frac{\pi M_e c^2}{e^2 \lambda^2} = 2.79\,10^{24}\ cm^{-3}\left(\frac{\lambda\left(\overset{o}{A}\right)}{200\ \overset{o}{A}}\right)^{-2} \qquad (24)$$

The index of refraction decreases at increased plasma density.

For a plasma column with a given radial density profile, in which the density decreases as a function of distance away from an axis (figure 6), the refractive index decreases as a function of the radius.

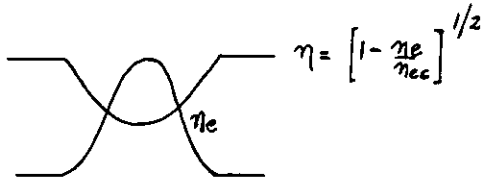

Figure 6 - Refractive index radial profile for plasma column with maximum density on axis.

In such plasma commonly encountered in x-ray laser situations, according to Snell's law of refraction, a ray propagating from a region of lower index of refraction to one of larger index of refraction will be bent away from the axis.

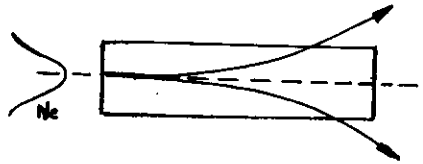

Figure 7 - Effect of refraction on x-ray propagation along a plasma column with radially decreasing plasma density.

London [18] has analyzed refraction in the case of a plasma with a density gradient in one dimension (x) (Figure 8). This assumption of considering all properties constant in the z directions is a good approximation in the case of plasma created by bombarding a solid target with a line focused laser.

Treating the density profile as parabolic, London computed the characteristic refraction length, L_r (typical distance in the z-direction a ray stays within the lasing medium before bending out), and the refraction angle ϕ_r:

$$\eta_e = \eta_o\left[1 - \left(\frac{x}{L_x}\right)^2\right]$$

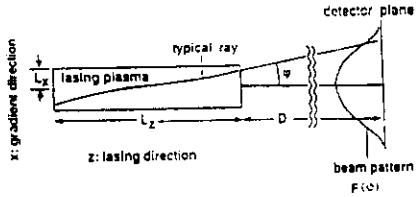

Figure 8 - Schematic diagram of x-ray laser and beam pattern showing the coordinate system and dimensions. Properties are assumed constant in the y-direction. After R. London, ref [18].

$$L_r = L_x \left(\frac{\eta_c}{\eta_o}\right)^{1/2}$$

$$\phi_r = \sqrt{\frac{\eta_o}{\eta_c}}$$

In the far field, refraction can cause sometimes sidelobes in the beam pattern. Beam patterns for lasers computed by London for parabolic electron density and gain profiles are shown in figure 9 for values of L_z/L_r between 1 and 4.

$$G_r = g_o L_r$$

and the L_z/L_r ratio.

Results are shown in figure 10. Two major cases are encountered. When $G_r>1$, exponential growth of the laser power is maintained. In contrast, when $G_r<1$ refraction dominates to the point that puts a limit to the exponential growth and power reaches a constant value for large lengths (curve corresponding to $L_r= 0.125$ in figure 10).

In the first case, when $G_r>1$, the refraction acts to reduce the effective gain coefficient, and for long plasma lengths, ($L_z>L_r$), the power increases with an effective gain coefficient

$$g_{eff} = g_o - \frac{1}{L_r}$$

In the same paper London also computed beam profiles for constant and quartic gain profiles. He also analyzed the length dependence of the on axis radiation flux for cases corresponding to several different values of the refraction length. Results were expressed as a function of a parameter, the refraction gain-length defined as:

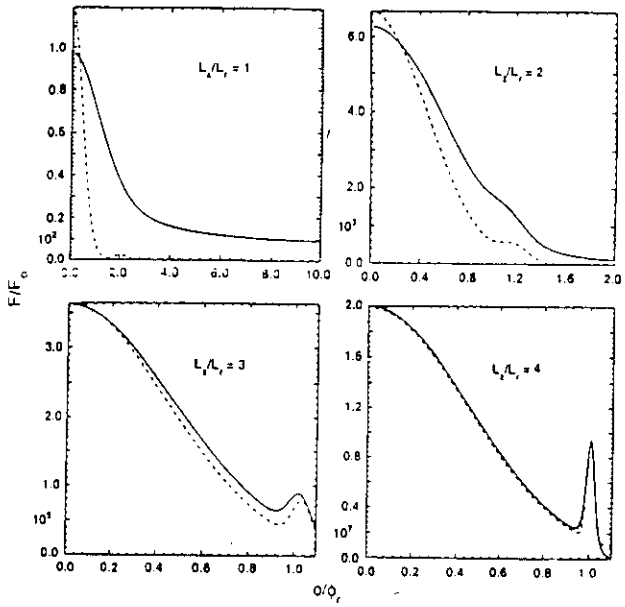

Figure 9 - Beam profiles for laser amplifiers with parabolic electron density and gain profiles. All cases are for $g_o=5/L_r$. The four figures are for different values of L_z/L_r as indicated. The solid curves are from numerical integrations and the dashed curves are from analytical approximation. After R. London, ref. 18.

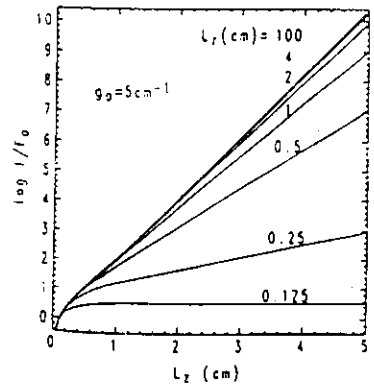

Figure 10 - On-axis flux versus length for several values of the refraction length, from ref. 18

In the case of a plasma with cylindrical symmetry, (density gradients in two dimensions) refraction can be shown to cause similar effects. In this case, refraction causes a far field beam profile with an annular shape. When observed through the slit of an spectrograph, appears as two symmetric sidelobes. In the cylindrical case, of interest for discharge pumped lasers and axially pumped laser plasmas, again two cases appear when analyzing the dependence of the laser power with plasma column length [19]. When $G_r > 2$ the exponential growth is not stopped by diffraction, and the laser power increases with an effective gain coefficient given by

$$g_{eff} = g_o - \frac{2}{L_r}$$

In the opposite case when $G_r < 2$, refraction imposes a practical limit the maximum practical plasma column length by limiting the exponential growth.

Several techniques, including the use of curved laser targets and the use of a pre-pulses have been recently developed to reduce the detrimental effects of refraction. These experiments are discussed later in the text.

TRAPPING OF LOWER LEVEL RADIATION

In many practical x-ray laser systems, for a given plasma column diameter, another limitation to the plasma density is determined by the increased opacity of the radiative transition responsible for depopulating the laser lower level. Re-absorption of photons spontaneously emitted by lower laser level atoms by ground state ions of the specie of interest, normally present in large abundance, can effectively increase the lifetime of the lower laser level. This effect decreases the population inversion in lasers with "caw" excitation mechanisms, that rely on the fast radiative decay of the lower level (figure 7). The magnitude of this effect is taken into account by multiplying the A_{10} coefficient by the "escape factor"$G(\tau)$, such that

A_{10} *effective* $= A_{10}\, G(\tau)$
where $0 < G(\tau) < 1$

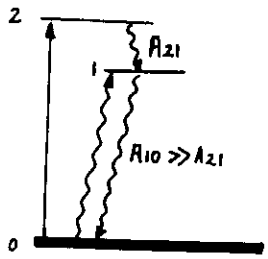

Figure 11 - Schematic representation "cw" laser excitation mechanism in which $A_{10}>>A_{21}$ helps to create large population inversions. Reabsorption of the lower level radiation by abundant N_o ions increases the N_1 population and decreases the gain.

In the limit case of $G(\tau) = 1$ we are back to the case of an optically thin plasma, with negligible absorption, in which all photons emitted by the laser lower level rapidly exit the plasma. The limit of a completely opaque plasma $G(\tau) = 0$, corresponds to the case in which the radiative lifetime of the lase lower level becomes infinite.

The escape factor depends on the opacity at line center, τ_{vo}, defined as the product of plasma thickness d and the absorption coefficient K

$$\tau_{vo} = K_{vo}\, d = N_o\, \sigma_{vo}\, d \qquad (27)$$

and which determines the distance in which a beam of photons of frequency is absorbed in a plasma according to

$$I(d) = I_o e^{-\tau_{vo}} \qquad (28)$$

where σ_{vo} is the absorption cross section and N_o is the ground state ion density.

For the case of a Doppler broadened line, in a static plasma, is τ_{vo} [3]

$$\tau_{vo} = 1.1\, 10^{16} \lambda_{vo}\, N_o\, f_{12}\, N_o \left(\frac{M}{k_B\, T_i}\right)^{\frac{1}{2}} \qquad (29)$$

where M is the atomic mass number, $k_B T_i$ is in eV, λ in Å, and d and N_o in cm and cm^{-3} respectively.

The dependence of $G(\tau)$ on τ for such static plasma is shown in figure 8, illustrating that the effect on destroying the gain could be dramatic, limiting for a selected density the plasma radius to very small values.

For example, for the λ = 182 Å recombination laser in H-like Carbon, in which the laser lower level depopulates by radiative decay at λ =37.7 Å the ground state from equation (29) using

$F_{01} = 0.42$
$M = 12$ AMU
$k_B T_i = 20$ eV

$$\tau_{vo} = 1.2\, 10^{-15} = N_o d \qquad (30)$$

for a ground state ion density of $N_o = 10^{18}$ cm^{-3}, τ_{vo} reaches unity at a diameter of d = 8μm. The size is further reduced for shorter wavelength lasers, that operate at higher densities, putting a very important constraint on the plasma density-diameter product.

Fortunately, the constraints are not as dramatic in many practical laser systems due to a reduction of the optical depth at line center by Doppler de-tuning of the absorption line resulting from plasma velocity gradients. The optical depth reduction has been analyzed by Sobolev [20](for astronomical purposes, and by Post [21] and London [22] for x-ray laser plasmas. This effect can be very significant in reducing radiation trapping. For example in practice, gain has been observed in 182 Å for plasma columns of d > 100 μm, a value much larger than computed using (30).

AMPLIFICATION DIAGNOSTICS AND GAIN MEASUREMENT TECHNIQUES

Several different diagnostic techniques can be used to observe the effects of amplification, several of the most useful are described below.

MEASUREMENT OF LASER BEAM POWER AS A FUNCTION OF PLASMA LENGTH

The most convincing evidence of amplification in an unsaturated gain medium is the measurement of an exponential growth of the intensity as the plasma length is incremented (Fig 12)

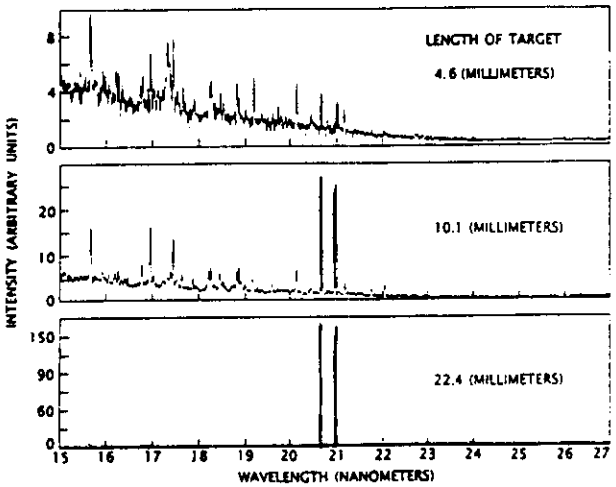

Figure 12 - Axial spectra form a Ne-like Selenium soft x-ray amplifier as a function of plasma column length. From ref.26.

This is achieved by monitoring the laser line intensity on axis, and changing the plasma column length while maintaining the pumping power density and other plasma properties constant. This can be easily done in the case of plasma generated by line focusing a laser on a target using a cylindrical lens. In this case, the different fractions of the pump beam are blocked, while maintaining the other parameters constant. A series of on axis spectra of a Selenium plasma, corresponding to the first successful collisionally excited x-ray laser experiment, conducted at Lawrence Livermore National Laboratory in 1984 by D. Matthews et al. [1] is shown in figure 13. In the 1cm long plasma the J=2-1 laser transition of Ne-like Selenium, which are relatively weak transitions in the absence of amplification are of similar intensity than strong spontaneous emission lines from surrounding ion species. The effect of amplification is dramatically evident in the following spectra corresponding to longer plasmas.

These type of measurements, utilizing the Linford formula, that does not require an absolute calibration of the spectral response of the detection system, is most useful because allows a direct measurement of the effective gain coefficient from a plot of the integrated line intensity as a function of plasma length. Figure 13 is such a plot for the J=2-1 of Ne-like Selenium, resulting from measurements conducted at the NOVA laser facility at Lawrence Livermore Laboratories. The gain of several optically pumped lasers using solid slab and foil targets has been measured in this way [9,10]. The same technique was recently utilized to measure gain in the first demonstration of large amplification in a discharge created in the J=0-1 line of Ne-like Ar at 46.9nm, conducted at Colorado State University using a fast capillary discharge [7]. Spectra corresponding to plasma columns 3, 6 and 12cm in length, are shown in figure 14. In this experiment the pumping conditions were maintained constant by maintaining both the amplitude and period of the current pulse constant as the length of the plasma was changed. The corresponding plot of integrated line intensity as a function of plasma column length is shown in figure 15. These first experiments in a discharge pumped Argon plasma yielded a gain coefficient of 0.6 cm^{-1} and a gain length product of 7.2 for a 12cm long plasma column. Subsequent experiments, discussed later in these lectures reached gl ~ 14 [23].

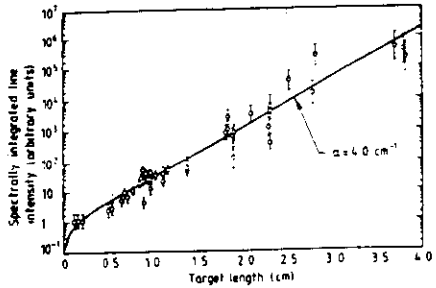

Figure 13 - Spectrally integrated intensity of the 206Å line of Ne-like Se as a function of plasma length. From ref. [26]

Another evidence of gain in this experiment, besides the clear exponential increase of the laser line intensity as a function of capillary plasma length is also observed in the spectra of figure 13. This is the relative change in intensity corresponding to two adjacent lines of the same ionization specie. In this case, the 46.9nm 3p-3s laser line and another Ne-like Ar line at 48.5nm, a 3d-3p transition that is computed not to have gain.

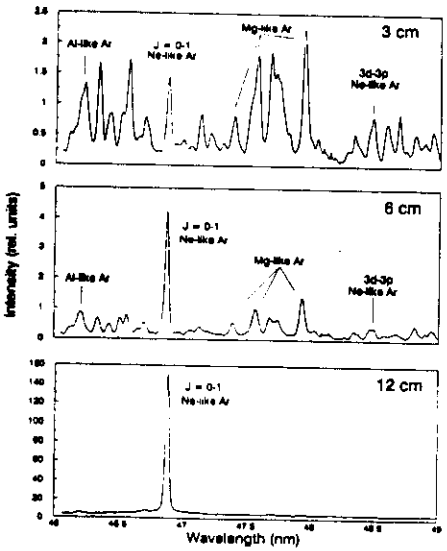

Figure 14 - Axial spectra from Argon capillary discharge as a function of plasma length. A dramatic increase in the intensity of the J=0-1 line of Ne-like Ar is observed. From ref. 7.

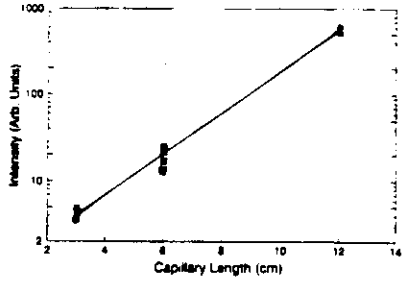

Figure 15 - Integrated line intensity of the J=0-1 ArIX line as a function of capillary plasma length. A fit to Linford formula is shown. From ref. 7.

In the absence of amplification, or for small gl, the ratio of intensities between the two lines is computed to be less than 5. First, for the 3cm plasma the two lines have comparable intensities. However, for the 12cm plasma column, the ratio

$$\frac{I_{46.9nm}}{I_{48.5nm}} > 300$$

a clear evidence of amplification.

RATIO OF LINE INTENSITIES OF AXIAL TO RADIAL EMISSION

Evidence of amplification can also be obtained from the relative intensities of axial and radial spectrum. For sufficiently small radius, typical of x-ray lasers for the reasons described in the previous pages, stimulated emission is negligible in the radial direction and consequently, a laser line will not be enhanced compared with other lines in this direction. For significant gains, the axial spectra should, in comparison, show the line enhancement. The measurement requires two spectrographs (axial and radial) and for a quantitative estimate of the gain, a relative calibration of the sensitivity of the instruments is required.

Evidence of amplification, obtained by this method for the LLNL Ne-like Selenium laser is illustrated in figure 15.

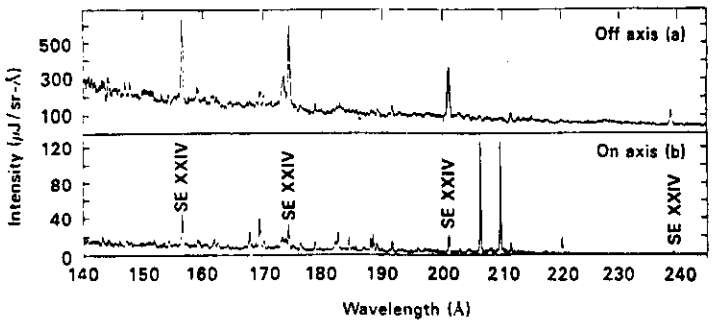

Figure 15 - Off axis and axial spectra from the plasma of a Selenium soft x-ray amplifier. From ref. 1.

The ratio of axial to radial line intensities was also utilized. As evidence of amplification in the first report of large gain by plasma recombination in the 3-2 line of Hydrogen like Carbon, conducted at Princeton [36]. Figure 16 shows the transverse and axial spectra corresponding to this experiment in which a carbon plasma was generated by bombarding a carbon target with a powerful (300J, 75ns) CO_2 laser [2].

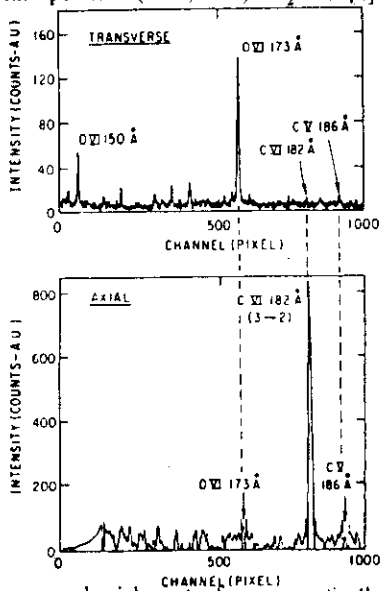

Figure 16 - Transverse and axial spectra from magnetically confined carbon plasma for a carbon disk target with 4 carbon blades. The laser energy was 500J. Ref. 6.

DOUBLE PASS AMPLIFICATION AND CAVITY EXPERIMENTS

A clear demonstration of amplification in visible lasers is the dramatic output beam that arises when an optical cavity is utilized. The use of such cavities is not yet possible in soft x-ray lasers, mostly due to the short lifetime of the gain. However, double pass (utilizing one normal incidence mirror) and multiple pass experiments are possible.

In a double pass experiment, the double pass integrated intensity of the laser line can in principle be expected (in the absence of gain saturation or large refraction) to be more intense than the single pass intensity by

$$\frac{I_{2\,PASS}}{I_{1\,PASS}} \propto R_1\, c\, e^{R_1 \ell}$$

where R_1 is the reflectivity of the mirror and C is a coupling constant that takes into account the fraction of the reflected beam that is effectively re-injected in the gain volume. An early experiment utilizing a normal incidence mirror with 12% reflectance, was conducted at Princeton in the 182 Å CVI recombination laser [2]. Double pass and triple pass amplification experiments were also conducted at LLNL [24,25], later at several other laboratories world wide [10, 24,25]. The time resolve evolution of the laser intensity is a triple pass experiment conducted at LLNL utilizing a normal incidence mirror and a beam splitter is shown in figure 17.

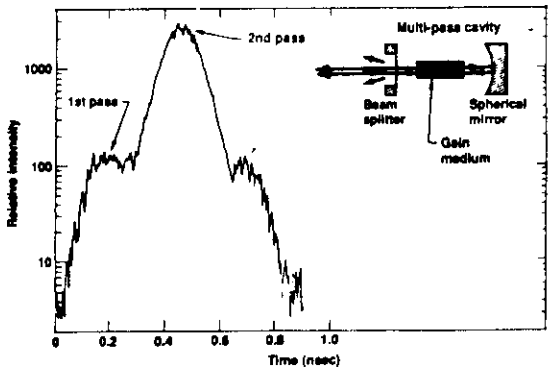

Figure 17 - Time resolved multipass cavity output at 206.3 Å in Ne-like Se. Total cavity length was 8.5cm. The gain medium was 2cm long. The reduced amplification for the third and higher number of passes was due to the short gain lifetime. From Ref. 25.

Each one of the lobes in the temporal evolution of the intensity is attributed to the first, second and third passes of the radiation through the amplifier. The second pass, as expected, is measured to be significantly more intense than the first. The smaller intensity of the third pass is attributed to the termination of the gain, that lasts only for the time of the pumping pulse, approximately 500ps. Such experiments are clear confirmation of amplification, and also serve to obtain important increases in the amplification, as the case of experiments conducted in collisionally excited lasers at LULI in France, where the second pass intensity was measured to exceed the first pass by a factor of about 80 [10]. It is nevertheless, not simple to obtain a measurement of the gain coefficient from a double pass experiment as it is difficult to accurately measure the coupling factor C.

LASER POPULATION EXCITATION MECHANISMS AND LASER DEVICES

While innovative excitation mechanisms will undoubtedly play a significant role in the future as x- ray lasers advance towards shorter wavelengths, today's soft x-ray lasers utilize excitation mechanisms that are extrapolations of their visible and ultraviolet atomic and ionic laser counterparts. Moreover, while a considerable number of population inversion mechanisms have been proposed, all successful experiments to date can be reduced to two of them: collisional electron excitation and collisional (three body) recombination. The generation of amplification by photopumping with soft x-rays has also received considerable theoretical and experimental attention, but in this case the best results to date consist of evidence of population inversions, but not of any significant amplification in the soft x-ray region. Do to our time constrain this lectures will focus in two experimentally successful ones. In the following section we will also review several variations and different implementations of these mechanisms.

COLLISIONAL ELECTRON EXCITATION

In this mechanism , schematically illustrated in figure 20 the laser upper level is excited by direct electron impact collisions between ions and electrons:

$$e(fast)+A^Z \longrightarrow A^{Z*}+e(slow)$$

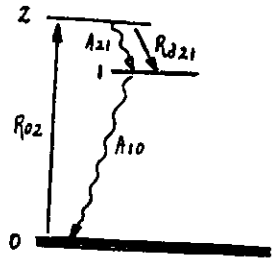

Figure 20 - Schematic energy level diagram of collisionally excited laser. The laser upper level is excited by direct electron impact excitation from the ground state of the ion. The laser lower level is rapidly depopulated by spontaneous emission.

This is the excitation mechanism by which the visible and ultraviolet argon ion laser lines are excited, the atomic copper vapor laser and many other successful infrared, visible and ultraviolet lasers work. Its use for the generation of soft x-rays was first proposed by ROC. Elton [28], and by Zherekhin, Koshelev and Letokhov [29], who first described the possibility of obtaining an inversion between the $2p^5 3p$ and $2p^5$ 3s levels in neon-like ions. Vinogradov and Shlyaptsev refined the early theoretical description [30]. This is the isolelectronic sequence the one that has been more successfully exploited to date. The first clear demonstration of large amplification was achieved at Lawrence Livermore National Laboratory in 1984 [1]. Significant success has also been obtained by collisional excitation of Nickel like ions [9,26,49], that for a given value of Z lase at shorter wavelength than there neon-counterparts. Large amplification was also recently demonstrated in Palladium-like Xenon. The collisional excitation mechanism is the only one to date that has allowed the amplification levels necessary to achieve gain saturation. In all cases the lasing ions have a full electronic shell, characteristic that makes them abundant over a large range of plasma parameters . This is importance, because the gain and the duration of the laser pulse depend of the abundance and on the extent of their existence on plasma parameter space. It also makes it easier for experiments to obtain and reproduce the plasma conditions necessary for amplification.

LASING IN NEON-LIKE IONS.

As mentioned above the first successful and reproducible experiment of large amplification in Ne-like ions was conducted at LLNL in 1984, in Neon-like Selenium [1]. In the following decade a very large number of elements of that isoelectronic sequence, ranging from chlorine to silver have been demonstrated to lase. An energy level diagram for Neon-like selenium is given in figure 19. Several 3p-3s lines can present gain and be amplified. The diagram shows the strong J=2-1 laser lines observed in the first Se experiment at 206.4 Å and 209.8 Å . The J=0-1 line theoretically predicted to have the largest gain, but not observed in the original LLNL experiment , is also shown. While the diagram and the discussion that immediately follow focus on selenium, the general
considerations are also valid for other neon-like lasers (taking into consideration of the necessary scaling of the plasma density, temperature, etc.).

The 3p levels, which do not radiate to the ground state of the ion, are strongly excited by 2p-3p monopole electron collisions . The 3p levels are also strongly coupled to the 3d states by electron collision, at a rate the can exceed by 10-300 times that of the spontaneous radiative decay rate to the 3s laser lower levels. The lower laser levels are depopulated by strong radiative decay the ground state of the ion, provided the plasma is optically thin in the radial direction. A dense plasma, with a large electron temperature, of about 1/3 the excitation energy of the laser upper level is required for the generation of large population inversions.

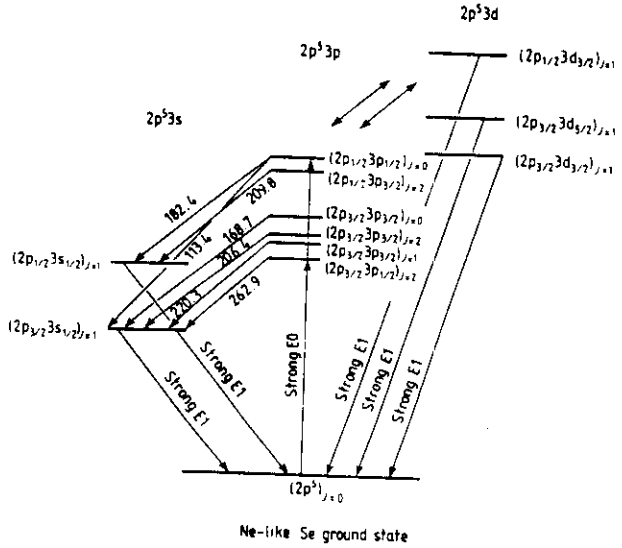

Figure 19 - Simplified energy level diagram for neon-like selenium. The originally observed strong J=2-1 laser lines at 206.4Å and 209.8 Å , and the J=0-1 laser line at 182.4Å are shown with other lines of interest. Reproduced from Ref. 26.

NE-LIKE SELENIUM EXPERIMENTAL RESULTS.

In the original LLNL selenium experiment the laser gain medium was generated by focusing two opposing multi-kilojoule green laser beams into a target made of a thin layer (750Å thick) of Se deposited on one side of a thin Formvar substrate [1]. The pump pulses had a pulsewidth of about 0.5ns, and a focused intensity of the order of 5 10^{13} W/cm^2 This exploding foil target configuration excited by two opposing line focused beams was designed as an attempt to minimize undesirable refraction effects by creating a more smoother electron density profile as compared to that created with slab targets. Schematic representations of the foil target and experimental set up of the LLNL Nova two beam chamber are shown in figure 20. Following irradiation by the pump laser these targets explode and produce a long uniform plasma column with a peak electron density of 3-5x10^{20} cm^{-3} at the time of the peak of the optical pulse, with a temperature of about

900eV, and with a distribution of ion charged states clustered around the Ne-like ionization stage.

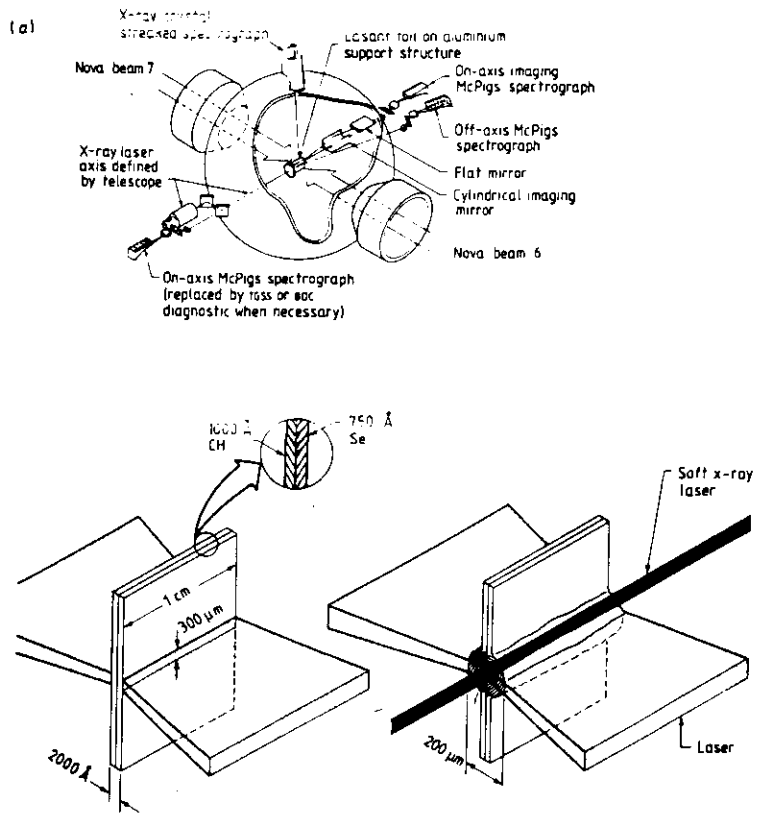

Figure 20 - a). Experimental set-up at the Nova two beam Chamber, showing the x-ray laser axis and diagnostics orientation. b) Schematic of the exploding foil target used in the Ne-like Selenium experiments. When irradiated by the Nova laser, the target explodes, producing a long plasma of characteristic dimension 200um in the transverse direction. Te=1000eV, Ne=4 10^{20}cm^{-3}. From Ref. 26.

The plasma produced when the foil is irradiated is diagnosed with a variety of instruments. Two grazing incidence vacuum spectrographs are shown to be used to observe the plasma on axis (In the original selenium experiments one of instruments was substituted by a transmission grating and a streak camera). The on-axis interments were used to measure the variation of the line intensity as a function of target length. In addition, a third grazing incidence spectrograph was placed on-axis and used to confirm the existence of gain by comparison of the line enhancement observed in the on-axis spectra as compared to the off-axis spectra.

In the first report, in which targets up to 2.2 cm were used , a gain length product of 6.5 was reported for the J=2-1 lines. In this experiment the J=0-1 line, which was predicted theoretically to have the largest gain, was not observe. However subsequent experiments showed lasing in this and other lines, with nevertheless lower gain [9,26]. An axial spectra of a neon-like selenium LLNL exploding foil target experiment is shown in figure 21. The observation of lower gain the J=0-1 line gave origin to what was named as the "J=0-1 anomaly", for which several explanations were proposed [3]. Only recently this problem was solved perhaps definitively, with the advent of experiments that utilize a laser pre-pulse (that precedes the major excitation pulse) to create smoother plasma profile, with reduced density gradients. In those experiments the J=0-1 line was observed to be the dominant line, in agreement with calculations.

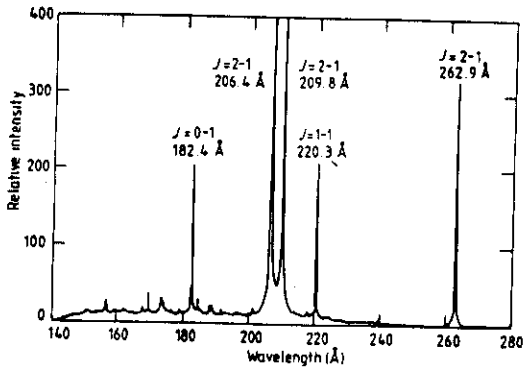

Figure 21 - Axial spectra of a Ne-like Se exploding foil target. The target was 2 cm long. The 206.4Å and 209.6Å lines are overexposed in order to allow weaker transitions to be clearly seen. From ref. 26.

More recently experiments conducted using targets up to 6.3 cm in length resulted in gain length products in excess of gl=25 [9] and in the observation of saturation of the gain as illustrated in figure 3a. Saturation is observed to occur at about gl=16. As

discussed below, gain saturation has also been obtained in lines corresponding to other neon-like ions.

The soft x-ray laser beam emerges from either end of the amplifier with a horizontal divergence of 10 to 15 mrad and a vertical divergence of about 20 mrad. The horizontal divergence of three of the Se x-ray laser lines is shown in figure 22a for a 2.8 cm long foil. The beam pattern peaks on the side of the foil axis that has been coated with selenium. Experiments with symmetric targets showed symmetric laser beams. The depression in the center of the beam pattern is due to density gradients, that refract the beam away from the foil axis.

The time history of the 206.4Å line is shown in figure 22 b, in relation with the duration of the pump laser pulse. The duration of the laser lines, 200ps in this experiment, is short as compared with the duration of non-amplified lines from surrounding ions.

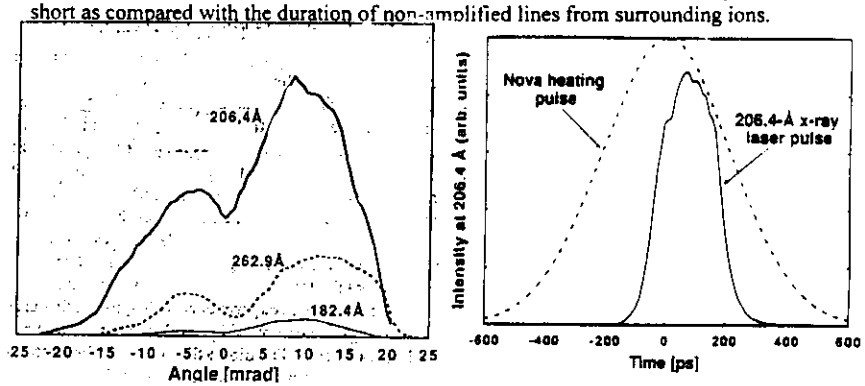

Figure 22 - a) Angular divergence of a Ne-like Se laser line. b) Time history of the 206.4Å laser pulse as detected with a streaked spectrometer. The dashed curve shows the time history of the 500ps Nova heating pulse. From Ref. 9.

Shortly after the demonstration of gain in Ne-like selenium, gain was achieved in Ne-like Y, copper, germanium and molybdenum [31b]. Since then, many elements ranging from Z as low as chlorine to as high as silver have been demonstrated to lase. In the last three years, the number of low Z neon-like lasers have greatly increased, with the use the pre-pulse technique discussed in the next section.

EFFECTS OF THE USE OF A PRE-PULSE IN THE EXCITATION.

A significant number of new laser lines in neon like ions were recently achieved utilizing a two pulse excitation technique described in the literature as the prepulse method [32,33]. In this scheme a plasma is created by lower energy prepulse that precedes the main pumping pulse by several nanoseconds. Subsequently, the main heating pulse that

follows provides the necessary energy to heat it and ionize it to the necessary stage. The main excitation pulse therefore interacts with a relatively low density target, that has a density of ions that is much closer to that require for lasing than a solid target. Simulations by Nilsen et al. [32] indicated that the pre-pulse is very efficient in making a larger and more uniform plasma that reduces the density gradients that are responsible for refractive effects.

This technique, first utilized to obtain lasing in Neon-like Titanium [34], has recently been extensibly utilized [35], in particular for low-Z Ne-like ions. Subsequently it has been used to obtain lasing in a large number of low Z Ne-like ions that have not been previously demonstrated to lase [36]. A list of transitions in Ne-like ions observe to lase utilizing a prepulse at the Max-Planck Asterix iodine laser facility is shown in Table I. Lasing in Z as low as chlorine was achieved at that facility utilizing the prepulse technique. The effect of the pre-pulse in the case of a Zinc laser is shown in figure 23 . The effect of the prepulse is most dramatic in the case of the J=0-1 line, which is not observed to lase in this figure in the absence of a the prepulse. Recently, the J=0-1 line has been observed to be the dominant line in elements ranging from titanium to selenium when a prepulse is present. Such experiments and the corresponding theoretical analysis point out to large d :nsity gradients in the region of gain for the J=0-1 line, as the source of the previously discussed J=0-1 anomaly in plasmas without prepulse. While the J=2-1 lines have inversion in the plasma corona, the J=0-1 line has maximum gain near the critical surface, and is therefore suffers more from refraction. The prepulse causes gradient smoothing and an extension of the amplification area.

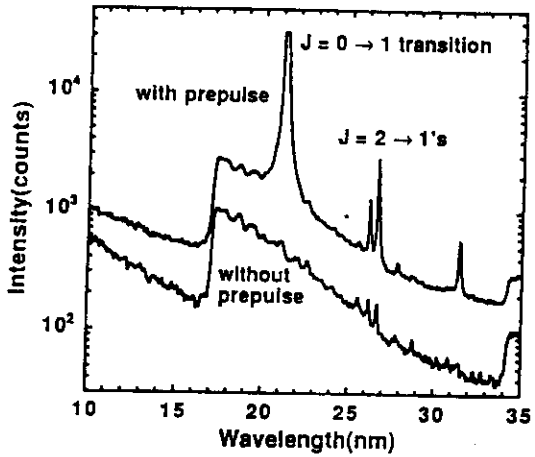

Figure 23 - On-axis time integrated spectra from 2.5 cm long Zinc targets with and without pre-pulse. Pre-pulse level 7.8%. of the main pulse. With the prepulse the J= 0 -1 line saturates the detector. From ref. 29.

Table I. Wavelengths (λ), gain coefficients (g), and gain lengths (gl) for the J=0-1 lasing observed in this work. The wavelengths are taken from ref. [15] An error bar of ± 0.8 cm^{-1} is estimated when error is not given, mainly due to the fluctuation in experimental conditions. The drive laser energy was 450±50 J. The intensity ratio of prepulse to main pulse under which the gain was measured is also given.

Ions	*Transitions*	*λ (nm)*	$I_{prepulse}/I_{main}$	*g* (cm^{-1})	*gl*
Ge^{22+}	E(0-1)[a]	19.6	1.5%	3.7±0.3	9.2
Ga^{21+}	E(0-1)	20.4*	15%	4.3	10.7
Zn^{20+}	E(0-1)	21.2	1.5%	4.5	11.2
Cu^{19+}	E(0-1)	22.1	1.5%	4.3	10.7
Ni^{18+}	E(0-1)	23.1	1.5%	4.3	10.7
	G(0-1)[b]	17.6	1.5%	-	-
Co^{17+}	E(0-1)	24.2	1.5%	-	-
	G(0-1)	19.0*	1.5%	-	-
Fe^{16+}	E(0-1)	25.5	1.5%	4.1±0.5	10.2
	G(0-1)	20.5	1.5%	2.3±0.5	5.7
Mn^{15+}	E(0-1)	26.9*	15%	4.3	10.7
	G(0-1)	22.1*	15%	2.5	6.3
Cr^{14+}	E(0-1)	28.5	15%	3.9	9.6
	G(0-1)	24.0	15%	3.0	7.4
V^{13+}	E(0-1)	30.4	15%	4.4±0.7	11.0
	G(0-1)	26.1	15%	5.0±1.1	12.5
Ti^{12+}	E(0-1)	32.6	15%	3.0	8.2
	G(0-1)	28.5*	15%	-	-
Sc^{11+}	E(0-1)	35.2*	15%	3.8	9.8
	G(0-1)	31.2*	15%	-	-
Ca^{10+}	E(0-1)	38.3*	15%	3.8	11.4
K^{9+}	E(0-1)	42.1*	15%	3.4	10.2
Cl^{7+}	E(0-1)	52.9*	15%	2.5	7.5

[a] $3p^1S_0$-$3s^1P_1$ transition
[b] $3p^1S_0$-$3s^3P_1$ transition

Table I - Laser lines in Ne-like ions obtained at the Max Planck Asterix laser facility using a pre-pulse. The wavelengths, gain coefficients and gain length observed are give. From ref. 36.

NICKEL-LIKE X-RAY LASERS.

The Nickel-like sequence of ions have been successfully utilized to demonstrate amplification at wavelength as short as 35.6Å. Nickel-like $3d^9$ 4d-$3d^9$ 4p lasers are direct analogs to the $2p^5$ 3p-$2p^5$ 3s laser transitions in Ne-like ions. The advantage of the Ni-like lasers is the lower pump power required to generate a given x-ray laser wavelength, making possible to achieve lasing at shorter wavelength with an available pump source. A goal for the development of x-ray lasers at shorter wavelengths has been the generation of bright coherent radiation near the carbon K absorption edge for the production of x-ray holograms and microscope images of living micro-organisms.

Ni-like x-ray lasers were first demonstrated in 1987 in a laser produced plasma of Eu, when gl=4 was obtained at 71.0 Å [37]. Subsequently the scheme was isoelectronically extrapolated to other ions and to wavelengths as short as 35.6Å in Ni-like Au. In the latter case, while gain was clearly demonstrated the maximum gl obtained was small. The Ni-like system is illustrated for Ta $^{45+}$ in figure 24, which shows the 4d-4p transitions observed to have gain in that particular ion. The 4d levels are populated through a combination of direct electron collisional excitation from the ground state of the ion, and from cascade from higher levels. As in the case of neon-like lasers , the laser lower level is rapidly depopulated by radiative decay to the ground state. The highest gain is observed in the J=0-1 line. Spectra for Ta foils are shown in figure 25a, in which the 44.83Å J= 0-1 line has about gl=8. The time history of the laser pulse is shown in figure 25b.

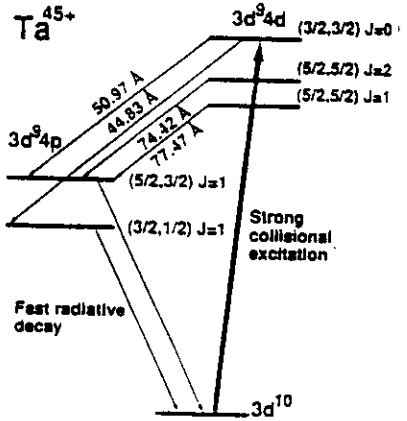

Figure 24 - Simplified energy level diagram of Ni-like Ta showing the four 4d-4p transitions that were observed in the experiments. The largest gain is observed in the J=0-1 line at 44.83Å. After Ref. 9.

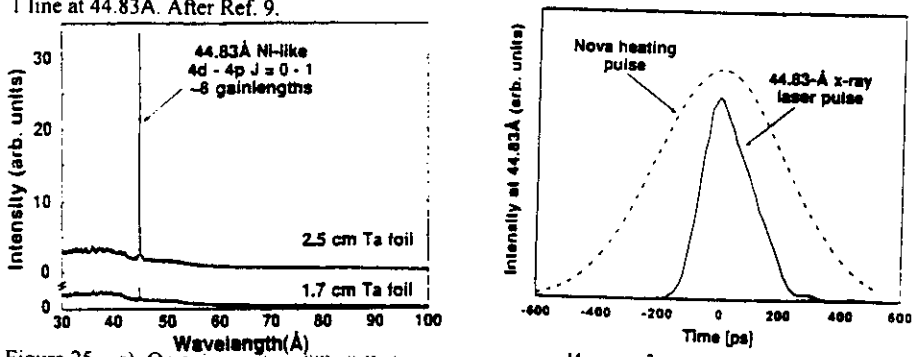

Figure 25 - a) On axis spectra of Ta foils irradiated at 2.4 10^{14} W cm^{-2}. b) Time history of the Ne-like Ta laser pulse. From Ref. 9.

More efficient excitation of lasers in Ni-like ions was recently achieved for lines in the 6 to 8nm region in the Institute of Laser Engineering at Osaka utilizing curve slab targets and multiple pulse excitation [38]. The first pulse acts as a pre-pulse and lasing is observed during the second and sometimes third excitation pulses. Gain was reported for several Ni-like lanthanide ions: Nd, Sm,Gd, Tb and Dy in the Gekko II laser facility using1.053 μm wavelength laser radiation. The 2.5cm long curved targets, utilized to compensate for refraction and maximize the extend of the gain region, were excited with multiple pulses with an energy of about 250J, which is an order of magnitude lower than previously reported for the Eu. The excitation pulses were 100ps duration separated by 40ps. Sequences of two or three laser pulses were used. Typical spectra showing the laser lines are shown in figure 26a. In several of the spectra two J= 0-1 laser lines are observe, but in all cases the longer wavelength line is dominant. The corresponding variation of the laser intensity with target length is shown in figure 26 b. The data corresponds to a gain coefficient of 3.1cm^{-1} and a gain length product of 7.8 for the 7.97nm line in the Nd ions with 250J of excitation energy per pulse. The laser output energy is estimated at about 1μJ , and the laser power at 10kW. The temporal profiles of the laser pulses respect to the plasma continuum emission (with is practically coincident with the pump laser pulses) is shown in figure 27.

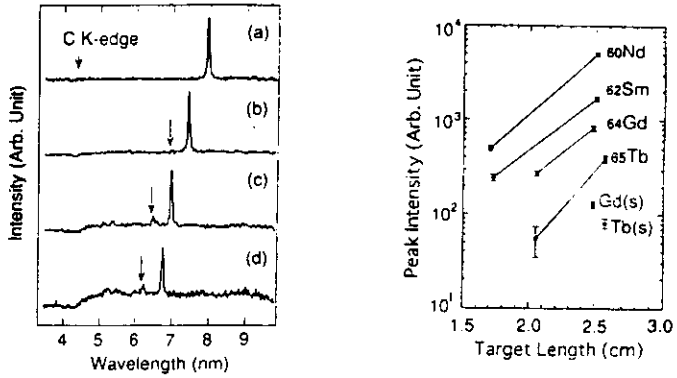

Figure 26 - a) Typical spectra of laser lines of Ni-like a) Nd, b)Sm, c)Gd and d) Tb obtained at the Gekko II laser facility utilizing curved targets and multiple pulse excitation. In some of the spectra two J=0-1 laser lines are observed. b) The relative peak intensity of the longer wavlength J= 0-1 lines as a function of target length. From Ref. 38.

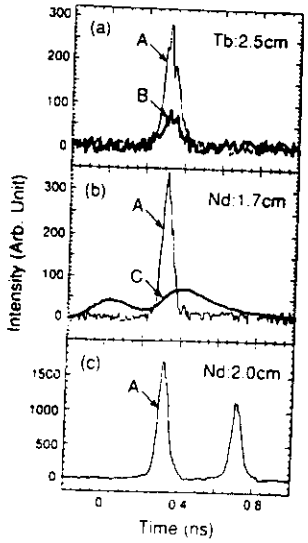

Figure 27 - Temporal profiles of the J=0-1 lines of Tb in a) and Nd in b and c). The notation A, B and C denote the temporal profile of the longer wavelength, shorter wavelength J=0-1 laser lines and the background x-ray continuum. In this case each of the pump pulses contained 130J and the separation pulse to pulse was 400ps. From Ref 38.

COLLISIONAL LASERS EXCITED BY OPTICAL FIELD IONIZATION.

Burnet and Corkum suggested an alternative way to excite electron excitation lasers: by optical field ionization (OFI) using high-intensity ultrashort optical pulsed [39]. In this method intense circularly polarized light is used to create both the highly ionized species and the hot electrons necessary to excite the laser upper level by collisional excitation. The ions are produced by tunnel ionization by the intense electric fields produced by the focused pump pulse. Tunnel ionization can fully strip the outer shell of complete shell atoms such as Ne-like and Ni-like species ions and simultaneously produce electrons with sufficient energy to excite collisionally the upper laser level For circularly polarized light the instantaneous ionization rate can be computed by the tunneling formula for static electric field [40]. Also, because. the ionizing femtosecond laser pulses are much shorter than any multiparticle interaction time, the electron energy distribution can be approximated by that calculated for isolated atoms. Theory predicts that electrons produced by tunneling ionization with circularly polarized light retain after the pump pulse has finished a kinetic energy equal to the quiver energy $\varepsilon = e^2 E^2/4mW^2$

Figure 28 shows the initial electron energy distribution calculated for argon when it is subjected to a 30fs pulse with an intensity of 10^{17} W/cm^2 [31]. The circularly polarized laser intensity required for the production of an ionization rate of 10^{14} s^{-1} for several species is illustrated in figure 29.

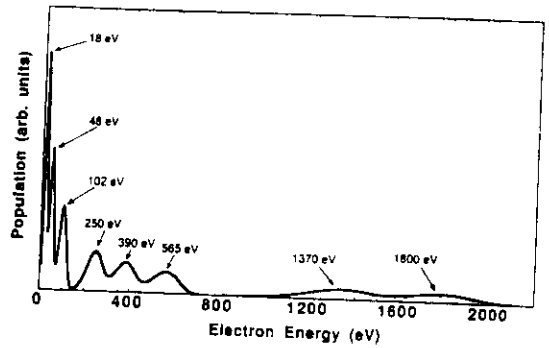

Figure 28 - Calculated initial electron energy distribution produced in Ar by a circularly polarized 30fs FWHM Gaussian pulse of peak intensity 10^{17} W/cm^2. From Ref. 40.

OFI collisional excitation lasers have the advantage of a cold ion temperature, and consequently a narrow laser linewidth and a high gain. The OFI collisional excitation scheme has potential for the development of compact soft x-ray lasers. Lemoff et al. have analyzed the implementation of femtosecond pulse driven, electron-excited XUV lasers in $\Delta N=0$ transitions in eight times ionized noble gases. They were also first in reporting lasing in an OFI collisionally excited system, in Xe-like Pd [14]. The experimental set up and the results obtained in these experiments are summarized in the section entitled "Table-top soft x-ray lasers". More recently the same group analyzed the possibility of utilizing $\Delta N=0$ transitions in Be-like ions, which would have the advantage of a more rapid scaling towards shorter wavelengths.

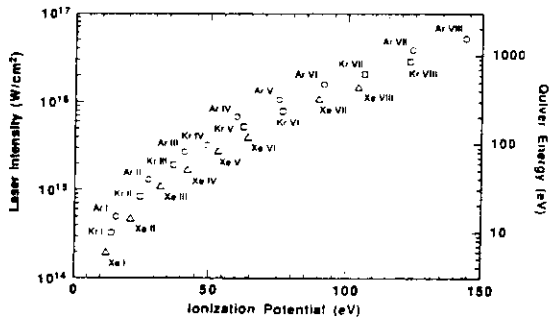

Figure 29 - Circularly polarized laser intensity required for the production of an ionization rate of 10^{14} s^{-1} in the indicated species. Also shown is the corresponding quiver energy at 800nm. form ref. 40.

RECOMBINATION LASERS

Collisional recombination is the other excitation mechanism that has been demonstrated experimentally for the excitation of soft x-ray lasers This mechanism for the creation of population inversion was first proposed by Guszenko and Shelepin in 1965 [41]. As in the case of electron collisional excitation, it was first demonstrated in the visible and infrared regions of the spectrum.

In this case the laser upper level is populated following the recombination of ions with charge z+1 with an electron through a three body interaction This type of reaction known as collisional or three body recombination preferentially populates highly excited states of the ion of charge Z, therefore allowing the generation of population inversion.

$$A^{Z+1}+2e \rightarrow A^{Z^*}+e$$

Notice that collisional recombination is the inverse process of collision electron ionization.

The process of generation of population inversion is schematically illustrated in figure 30. Conservation of energy favors the excitation of highly excited states in ion Z. For these levels collisional electron de-excitation dominates over radiative decay, and the population of these levels is rapidly transfer to levels of lower energy. Since collision electron de-excitation is inversely proportional to the energy difference between the levels, the electronic cascade reaches a level at which electron de excitation is no longer dominant over radiative decay. At this point a bottleneck is produces in the de-excitation process and a population inversion is created respect to a lower level, most commonly de-excited by very rapid radiative decay to the ground state of the ion.

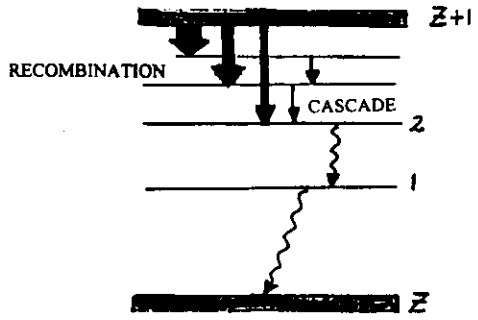

Figure 30 - Schematic representation of energy level diagram showing the generation of population inversion by collisional electron-ion recombination and by electron collisional de-excitation cascade.

The collisional recombination rate, R_{recom}, is proportional to the square of the electron density, as the reaction above suggests, and is extremely sensitive to the electron temperature. Classically, it is shown to depend of this parameter as $Te^{-4.5}$. Therefore, to have a high recombination rate, and therefore a large population inversion, a very dense, cold plasma is required. It seems a contradiction to simultaneously demand the requirements of a very highly ionized plasma and a very cold electron temperature. In practice, the problem is solved by first generating a highly ionized, dense plasma by a heating pulse, and then by rapidly cooling it. By this method the plasma is hot during the excitation pulse, allowing for the generation of the required high population density of ions Z+1. The rapid cooling must cool the plasma to a sufficiently low temperature before the ions recombine. Therefore the required cooling rate is determined by the recombination rate. The plasma can be rapidly cooled by a rapid adiabatic expansion, by electron heat conduction to a nearby wall or colder plasma, or by radiation from higher Z ions introduced as impurities. All three cooling mechanisms, or combinations of them, have been utilized experimentally to generate gain at soft x-ray wavelengths by collisional electron-ion recombination.

It should be noticed that if initially all, or the great majority of ions of species Z are ionized, and if the cooling is achieved in times significantly shorter than the recombination time constant, large population inversions might be created respect to the ground state. This has the advantage of providing a method to amplify very short wavelength lines in species which are only moderately ionized. The advent of very powerful subpicosecond lasers have made possible, as discussed below, the recent demonstration of population inversions respect to the ground state of ions.

The first demonstrations of large amplifications by collisional recombination have however been realized using nanosecond laser excitation pulses. Some of these experiments are discussed below.

RECOMBINATION LASING IN THE 3-2 TRANSITION OF H-LIKE CARBON

Hydrogen like ions, as originally suggested by Gudzenko and Shelepin [41] have a very favorable atomic energy level structure for the generation of population inversions. In principle several transitions can be inverted. Most of the attention have focused in the 3-2 transition of these ions. In particular important efforts have been devoted to the demonstration and study of amplification in the 182 3-2 line of H-like Carbon.

Initial experiments demonstrated the generation of population inversions by bombarding solid carbon targets with high power laser pulses, and by cooling the plasma by adiabatic expansion [34,35]. The first report of large (gl=6) amplification corresponds to an experiment conducted at Princeton in 1984 [2]. In this experiment, schematically illustrated in figure 31, a 300J, pulse from a CO_2 laser with about 75ns pulsewidth was used to generate a carbon plasma column by bombarding a carbon solid target immersed in a solenoidal magnetic field. The plasma column generated by ablation of the solid target was heated by the laser pulse to generate a high density of totally stripped carbon

ions The magnetic confinement allowed to maintain a high election density while the plasma was cooled by radiation and by electron heat conduction to cooling blades placed in close proximity to the plasma. Large gain is observed when the plasma temperature drops below 20eV Numerical simulations indicate that the amplifications takes place in a 100μm-thick annulus approximately 1cm in length [6]. The amplification was observed by comparing the axial and side-on emission, as illustrated in figure 16.

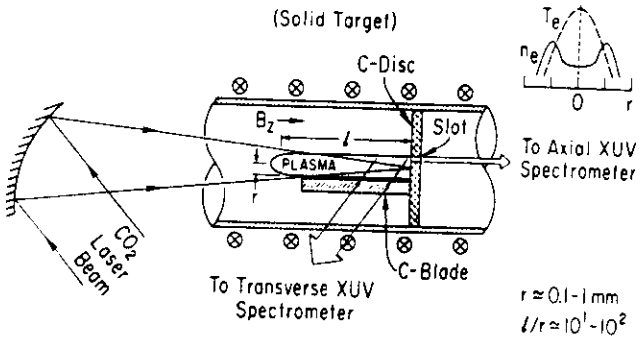

Figure 31 - Schematic representation of the experimental set up of Princeton soft x-ray laser experiment for recombination lasing in CVI in a magnetically confined plasma column. From C. Skinner et.al, ref. X

Successful amplification has been also demonstrated in a series of experiments in which line focus plasmas are cooled by free adiabatic expansion [36]. Amplification has also been demonstrate in other H-like ions such as O^{+7} and F^{+8}, and in the 4f-3d and 5f-3d lines of Li-like ions, such as Al^{10+} [42-43].

An advantage of the recombination scheme respect to the collisional excitation scheme is its more rapid scaling towards shorter wavelengths as a function of the ion charge. For example the H like C laser requires to initially ionize carbon six times to obtain large amplification at 182A, while to obtain amplification at the same wavelength exciting the J=0-1 line of Selenium requires to ionize selenium 24 times. Nevertheless to date recombination lasers have suffered the problem of not scaling adequately with plasma column length. Despite many attempts the largest gain length products achieve to date remains about gl=8. It has been suggested that the problem is related to the very high sensibility of the gain in recombination schemes to the variation of the plasma parameters, that is more pronounced for longer plasma columns. This limitation is nevertheless a current topic of discussion which requires further research. This issue must be resolved before x-ray recombination lasers can achieve their full potential.

RECOMBINATION LASING IN PLASMAS CREATED BY OPTICAL FIELD IONIZATION.

In the recombination lasers discussed above a hot plasma is initially created, and subsequently rapid cooling is achieved by either adiabatic expansion, electron heat conduction of plasma radiation. Optical field ionization again offers a new possibility of excitation for recombination lasers with potentially great advantages Burnett and Corkum have proposed that cold and dense plasmas for recombination lasers could be produced by focusing a linearly polarized high power density optical beam. In contrast to the case of OFI plasmas created by a circularly polarized beam, the temperature of the electrons produced can be low. This low electron temperature can be in principle obtained for a linearly polarized laser pulse as the electrons are compelled to return their quiver energy to the linearly polarized laser field. This method can therefore create plasmas that are simultaneously highly ionized and cold. A fully stripped plasma is produced on a time scale much shorter than their recombination time Amendt and Eder have analyzed the implementation of soft x-ray lasers based on OFI [44]. In order to realize OFI recombination lasers it is necessary to minimize undesirable electron heating originating from processes that occur in high intensity laser matter interaction. In situations in which these heating effects can be effectively minimized, this mechanism has the potential advantage of generating large soft x-ray amplification utilizing compact table-top pump lasers. Nagata et al. [45] reported gain by recombination in an OFI lithium plasma. These results are discussed in the section entitled "table top soft x-ray lasers".

TABLE TOP SOFT X-RAY LASERS.

While the pioneering experiments conducted at large laser facilities have clearly demonstrated amplification at many wavelengths ranging between about 35 A and 500A, in many cases generating very powerful x-ray beams, the widespread use of x-ray lasers in applications requires the development of more compact and affordable lasers sources. Such type of lasers, often called "table top " soft x-ray lasers have recently received considerable attention. The most significant progress have been achieved in the last two years , when both discharge pumped as well as laser pumped devices that fit in the table top category have achieve large gl products.

OPTICAL FIELD IONIZATION LASERS. RECOMBINATION LASERS.

Nagata et. al [45] recently reported the observation of gain in the 13.5nm 2-1 transition of H-like lithium in an OFI plasma. A very cold (approximately Te=1eV) plasma was realized by irradiating a pre-formed singly ionized lithium plasma with a 0.5ps KrF laser focused to an intensity of 10^{17} cm^{-2}. In order to produce the initial Li^+ plasma a 20ns KrF laser pulse with an output energy of 200mJ was line focused onto a rotating lithium target located into an evacuated chamber. After a certain delay time a linearly polarized 500fs KrF laser pulse with an energy of 50mJ was focused at 0.5 mm from the target surface. The Lyman series emission from the H-like Lyman series was detected with a flat field

grazing incidence spectrograph. A gain coefficient of 20cm^{-1} was reported. However, the plasma length was small, resulting in a small gain-length product.

More recently D. Korobkin et. al. demonstrated larger gain (g*l=5) in this line by increasing the active plasma length [61]. This was obtained utilizing a plasma waveguide generated by creating with a 5ns laser a plasma with a density gradient minimum on axis in a microcapillary tube. The excitation was produced by a 50mJ, 250fsec pulse from an excimer laser.

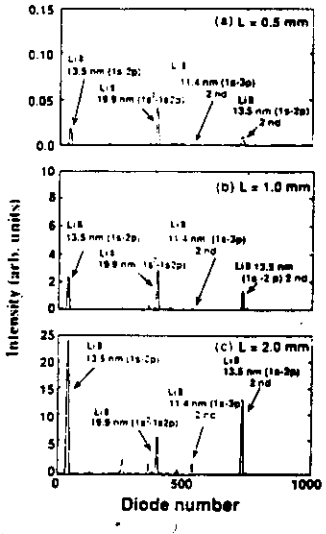

Figure 32 - On axis spectra from OFI Li plasma subjected to subpicosecond KrF laser excitation pulses for various plasma lengths. From ref. 45.

OPTICAL FIELD IONIZATION COLLISIONAL ELECTRON EXCITATION LASER.

As discussed in the section of collisional lasers OFI offers the possibility of realizing table top soft x-ray lasers. Lemoff et al. [ ] recently reported the first demonstration of an OFI collisionally excited laser in the 418A line of Pd-like Xe.

A femtosecond (40 fs) , 800nm pulse from a Ti:sapphire laser was used as a pump. The experimental set up utilized is schematically represented in fig.33. A gas cell provided with an entrance and exit pinhole of less than 500μm was placed inside the main vacuum chamber and served as the target. When the chamber contain 12 Torr of Xe, the pressure in the continuously pumped main chamber is kept to less than 2 10^{-3} Torrs. The pinholes are placed on translation stages to be able to change the gas target length. The pump laser is focused to about 3 10^{16} W/cm^2. The detection was accomplished utilizing a 1.5 meter grazing incidence monochromator and a dc biased multichannel plate.

Lasing at 41.81nm is evident in the 12 Torr spectra of figure 34, in which the laser line increases by more than two orders of magnitude respect to its intensity (and that of other lines) in the 3 Torr spectra also shown. Varying the target length provided a more direct measurement of the gain. Figure 34 shows the variation of the intensity of the 41.8nm laser line as a function of gas target length. The gain coefficient is estimated at 13.3 cm^{-1}

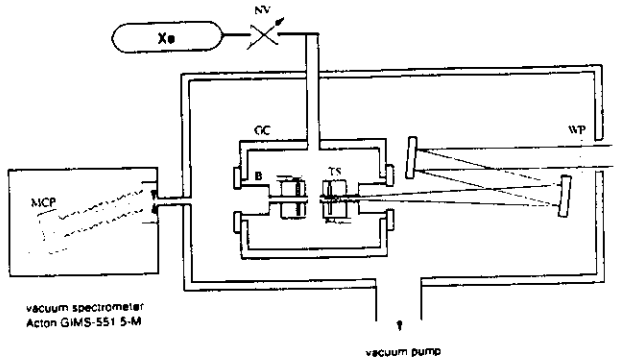

Figure 33 - Experimental set up utilized in OFI Pd-like Xe experiment. NV needle valve. Gc. Gas cell. WP wave plate. B. bellows. TS translation stage. MCP multichannel plate detector. From ref 48.

using the Linford formula, and the total gain of exp (11.2). When a Linford curve is fit only to the data from 3.9 to 7.4mm (dashed line) a better fit is obtained with a gain coefficient of 16.8 cm^{-1} and a gl=12.4 assuming a 7.4mm target. Scaling towards shorter wavelengths have been recently proposed by the Stanford group utilizing Be-like ions [46].

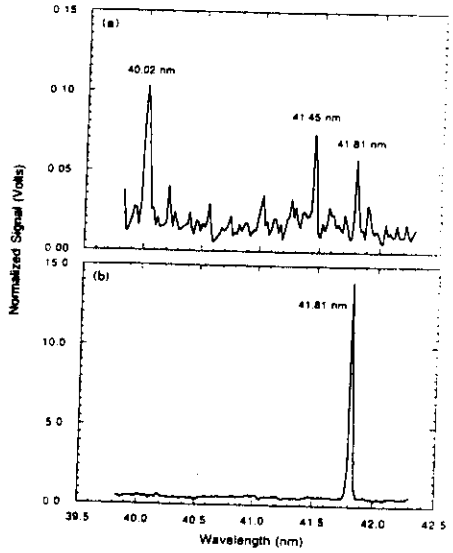

Figure 34 - Observed emission spectrum of Xe gas target excited by the femtosecond laser at an estimated target length of 8.4mm, and a pressure a) 3Torr and b) 12 Torr. The 41.8nm Pd-like Xe laser line is observed to increase in intensity by more than two orders of magnitude. From ref.14.

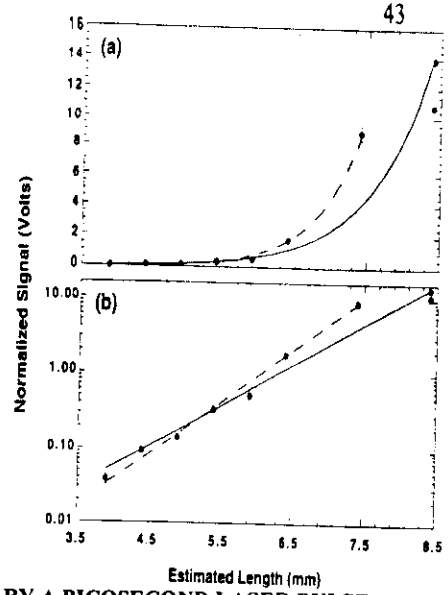

Figure 35 - Length dependence of the intensity of the 41.8nm Pd-like Xe laser line as a function of gas target length. Linford curves are shown to fit the data. The solid line is a fit to all the data. The dashed line is a fit to the data for 3.9 through 7.4mm targets only, a) linear scale. b) logarithmic scale. From ref.14.

NE-LIKE TITANIUM LASER EXCITED BY A PICOSECOND LASER PULSE.

Presently available terawatt table top infrared and visible laser systems create the opportunity to demonstrate amplification by electron collisional excitation in relatively compact set-ups. A gain length product of about 9 was recently reported in the 32.6nm J=0-1 line of Ne-like Ti, in a plasma excited by a terawatt table top pump laser, in experiments conducted at the Max-Born Institute in Germany. The gain coefficient reported of reached 19 cm-1, and is the result of non-stationary, transient inversion effect taking place in the plasma created by the picosecond laser. The experimental set up utilized in this demonstration, which makes use of two laser pulses, is illustrated in figure 36. A hybrid Chirped pulsed amplified Ti:Sa-Nd glass laser facility, that simultaneously produces a nanosecond and a picosecond laser pulse was employed. The two laser beams are orthogonally polarized to each other in order to recombine them with a polarizer prior to focusing them into the solid Ti target by a cylindrical lens focusing system. The excitation utilized an energy of up to 4J in the short picosecond pulse and up to 7J in the nanosecond pulse. The width of the focus was about 30μm and the plasma column length 2 to 5mm. The diagnostics system consisted of a transmission grating and a streak camera.

No laser pulse was observed as long as only one of both laser pulses was used. The first observation of gain was realized with short pulses of more than 2J and long pulses of more than 3J. The figure 3 illustrates the observed growth of the laser signal at 32.6nm as a function of plasma column length, for plasmas as long as 5mm. The temporal dependence of the soft x-ray laser pulse is shown in figure __b. The laser pulse has a duration of less than 20 picoseconds.

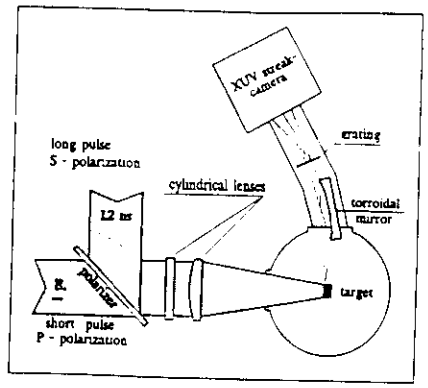

Figure 36 - Scheme of experimental set up for the Ne-like Ti utilizing the combination of a nanosecond and powerful picosecond laser pulses at the Max Born Institute. From ref.15.

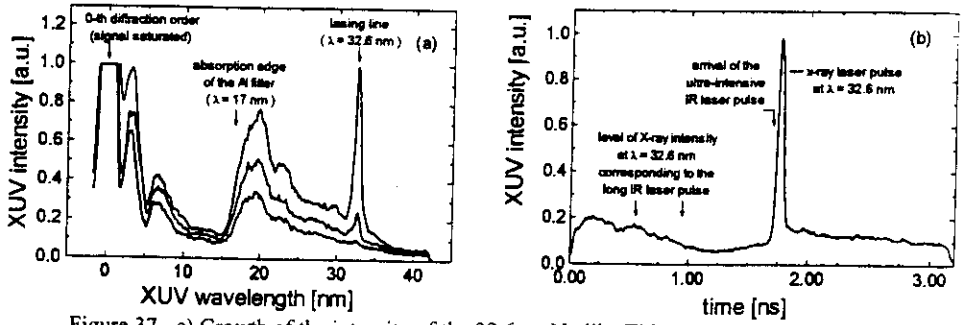

Figure 37 - a) Growth of the intensity of the 32.6nm Ne-like Ti laser line as a function of plasma length of 2, 3 and 5mm length at the moment when the 1ps pulse hits the preformed plasma. b) Time dependence of the 32.6nm radiation. From ref.15.

The measured integrated variation of the laser line intensity as a function of plasma column length is shown in figure 38 Despite the statistical fluctuations an exponential growth is observed for lengths at least as long as 3mm. The result represent a very important advance in reducing the pump energy necessary to excite Ne-like soft x-ray lasers It is likely that a large number of collisional laser transitions will be demonstrated to lase in similar systems in the near future.

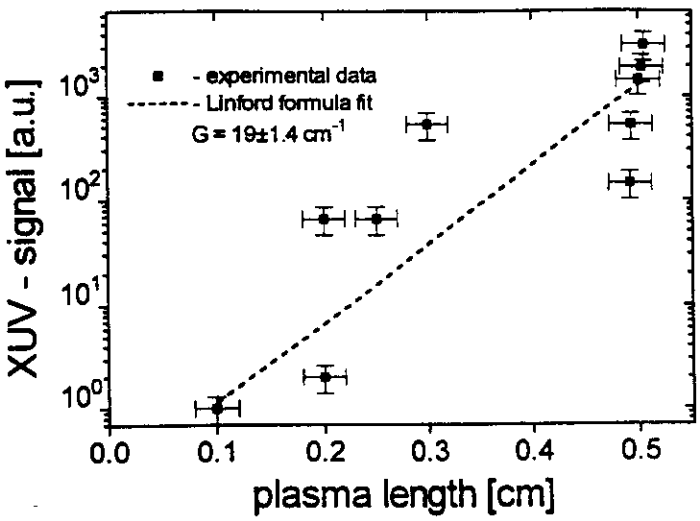

Figure 38. Intensity of the J=0-1 line of Ne-like Ti as a function of plasma column length. From ref 15.

PROSPECT FOR LASING IN A LASER CREATED PLASMA WAVEGUIDE.

A not yet demonstrated, but promising scheme for the development of efficient table-top soft x-ray lasers is the excitation of collisionally pumped and recombination lasers in a laser created plasma waveguide. In this scheme, investigated by H. Milchberg et al. the pump beam and the soft x-ray beam are both waveguided in a laser produced plasma channel for lengths that are much longer than those normally allowed in a dense plasma. The scheme has the advantage of potentially creating soft x-ray laser beams of greatly improved transverse coherence.

In this laser scheme two laser pulses are utilized. The first pulse generates a plasma refractive index channel through the hydrodynamic evolution of a laser breakdown spark in the selected ambient gas. The radial shock wave produced by the breakdown spark drives a shock wave in the ion density, leaving an ion density minimum in the axis, as illustrated in figure 39. Due to the electrostatic forces the electron density also develops a minum at the axis, that creates an index waveguide for the radiation of the pump laser, that will follow the laser pulse used to create the waveguide by a short selected delay. Milchberg has theoretically demonstrated that such plasma will also be a waveguide for the amplified x-rays.

minum at the axis, that creates an index waveguide for the radiation of the pump laser, that will follow the laser pulse used to create the waveguide by a short selected delay. Milchberg has theoretically demonstrated that such plasma will also be a waveguide for the amplified x-rays.

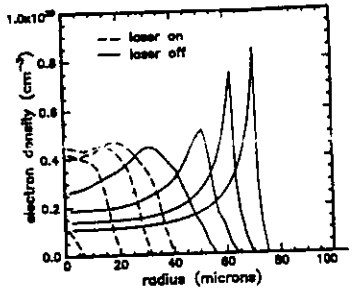

Figure 39 - Calculated electron density profile evolution in a nitrogen plasma excited an axicon lens. The laser pulse intensity is 5 10^{13} W/cm^2, Gaussian FWHM 100ps, spotsize 10μm and wavelength 1.06μm. the pulse peaks at 125 ps and ends at 250ps. The dashed curves for the laser on are separated by 50ps and those for laser off (solid curves) are separated by 500ps. The electron density profiles of the solid curves give origin to an index waveguide. From ref. 47.

Experimentally the waveguide is created by focusing the first laser pulse with an axicon lens A corner cube mounted on an optical delay rail provides a 1-15ns delay between the axicon pulse and the pump pulse, which is coupled into the waveguide by a lens. Preliminary experiments have demonstrated guided pump intensities of up to 2 10^{14} W/cm^2 over more than 2cm (70 Rayleigh lengths) Experiments are planned at the University of Maryland to demonstrate lasing in the 46.9 nm line of Ne-like argon , as well as in other laser transitions.

GAIN IN PLASMAS EXITED WITH LONGER PULSES FORM TABLE-TOP LASER PUMPS.

Amplification has also been reported in experiments employing table-top laser pumps that are characterized by longer laser pulses [Suck, hagel, hara]. A gain length product of abut 3 has been reported for the 204Å line of Ni-like Nb excited by a 2J, 60ps pulse at MIT [48]. The measure variation of the intensity versus target length is shown in figure 40

The same laser facility was used to investigate gain in recombination lasers. The best results to date were obtained in the 262Å (3-2 line) of H- like Boron. As in the case of the Princeton experiments ,a blade was added to the set up to enhance plasma cooling. The target set up for such experiment is shown in figure 41a. The results obtained, that correspond to a gain length product of about 4 are shown in figure 41b. The same group,

P.Hagelstein et al., has proposed end pumping configurations that are design to enhance soft x-ray laser efficiency [50].

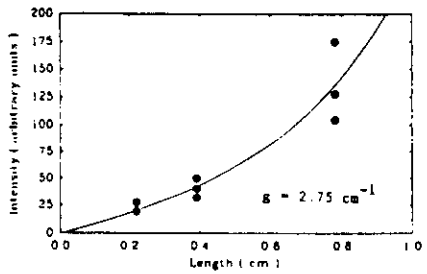

Figure. 40 - Intensity versus plasma length for the 204.2Å line of NI-like Nb. From ref. 48.

Similar pulse lengths from a 2-3 J laser and arranged in a pulse train are used by Hara et al. at the Toyota Technological Institute to investigate amplification by plasma recombination in Li-like Al.[51].

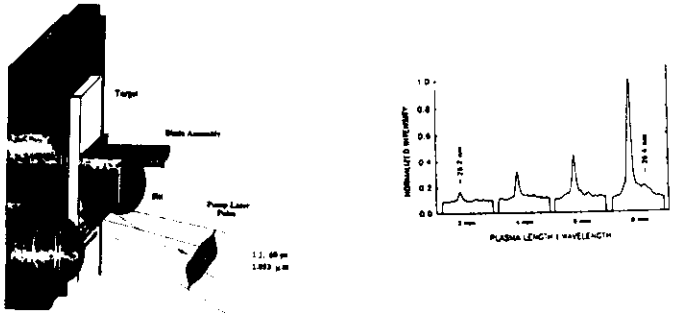

Figure 41 - a) Experimental set up and b) laser line intensity as a function of plasma column length, for amplification in H-like B at 262Å. From ref 49.

Work at Princeton by S Suckewer et al. has been devoted to the development of a more compact CVI recombination laser pumped by a Nd-glass with a pulse energy of less than 10J and a pulse length in the several nanosecond range. Several target configurations have been investigated. One of them, a two target configuration, is shown in figure 42. Gains of up to 7 cm-1 in 6mm long targets (gain-length product of about 4) have been reported for individual targets. No significant improvement in gl was observed using two

targets [52]. The latest efforts have included microcapillary targets, in which the laser is focused end-on in the capillary channel [52].

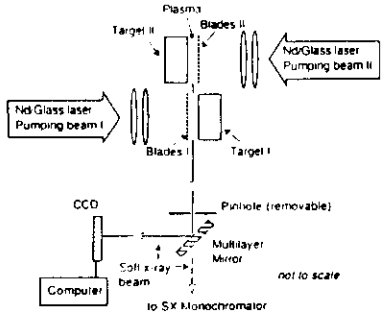

Figure 42 - Experimental set up of two target assembly to explore gain by plasma recombination in CVI using a table top laser pump. From ref. 52.

DISCHARGE PUMPED SOFT X-RAY LASERS

Alternatively, it has been recognized that direct discharge excitation of the soft x-ray lasing medium could result in increased efficiency and simplicity. However, despite the large success in the realization of discharge-pumped lasers at longer wavelengths, the problem of demonstrating large amplification at wavelengths below 100 nm had until recently remained unresolved. Figure 1 illustrates the rapid progress achieved in demonstrating lasers operating at increasingly shorter wavelengths during the first decade of discharge-pumped laser development, starting with the discovery of the helium-neon laser in 1961. However, after the demonstration in 1972 of lasing in hydrogen at 116 nm [53], further progress stalled for more than 20 years, until the experiments discussed herein. A major problem has resided in that shorter wavelength amplifiers require the creation of uniform plasma columns with increasingly hotter and denser plasma conditions. For example, while lasing in the blue at 488 nm can be obtained in singly ionized argon in a plasma with an electron temperature of about 5 eV and an electron density of $1x10^{14}$ cm^{-3}, lasing at 46.9 nm in the same element requires to ionize the atom eight times (to obtain neon-like argon), with more than an order of magnitude increase in the electron temperature, to about 80 eV, and nearly a five order of magnitude increase in the electron density, to about $1x10^{19}$ cm^{-3}. Whereas the requirements of high temperature and high density can be relatively easily met by high power discharges, that of simultaneously maintaining high plasma uniformity is not. Axial inhomogeneities and severe distortions in the plasma columns, produced by non-symmetric compressions and instabilities, often develop, destroying the amplification. To overcome these limitations Rocca et al. [54,55] have proposed and implemented the

excitation by fast capillary discharges. These discharges can produce hot plasma columns of small diameter by fast compressions starting from highly homogenous initial plasma conditions, which can result in more uniform plasma columns.

Utilizing a fast capillary discharge to create and excite neon-like argon ions, Rocca et al. have recently demonstrated for the first time large soft x-ray amplification in a discharge-created plasma, in the J=0-1 line of Ne-like argon at 46.9 nm [7]. The plasma column generated by fast compressional capillary discharges are also of interest to produce soft x-ray amplification by plasma recombination. Hereafter we focus our attention in discussing recent experiments conducted at Colorado State University, which have resulted in exponential gains up to approximately exp(14) in the 46.9 nm line of Ne-like argon.

AMPLIFICATION IN NE-LIKE ARGON

The discharge set up utilized to obtain amplification in Ne-like Ar is illustrated in Fig. 43. The pulse generator consists of a 3 nF liquid dielectric capacitor that is pulsed charged by a Marx generator. To generate the plasma columns, the capacitor is rapidly discharged through the capillary channel by a spark-gap switch. The radiation from the plasma was analyzed with a 2.2 m grazing incidence spectrograph having a 1200 l/mm, gold-coated grating.

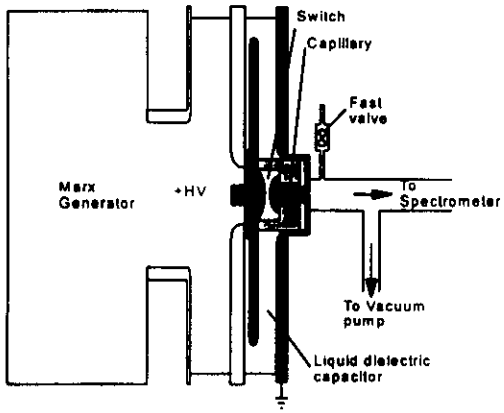

FIGURE 43. Schematic diagram of the pulse generator and capillary discharge setup. Ref. 55

The observation of large amplification in the 46.9 nm ArIX line, corresponding to a measured gain-length product of 7.2, was first realized in 4 mm diameter capillaries up to12 cm in length containing argon gas at a pressure of approximately 700 mTorr. The plasma columns were generated by a current pulse with a half-period of about 60 ns and a peak amplitude of near 40 kA. The fast current pulse rapidly compresses and heats up the plasma, to form a narrow column with measured length to diameter ratios exceeding 500:1. Toward the final stage of the compression, the plasma reaches nearly ideal conditions for soft x-ray amplification by collisional excitation in Ne-like and Ni-like ions. The value of the gain was determined by measuring the increase of the laser line intensity as a function of the capillary length. The laser pulse, which is observed to occur shortly before the time of maximum plasma compression, was measured to have a divergence slightly smaller than 6 mrad.

More recent experiments, conducted under optimized conditions in capillaries up to 16 cm in length filled with pure Ar gas further increased the laser intensity by more than two orders of magnitude. Gain coefficients up to 1.16 cm^{-1} were measured. Single pass amplifications up to exp(18) were achieved in a single pass through the amplifier, and effective gains up to exp(27) were measured in double pass amplification experiments utilizing an Ir mirror. This allowed to reach the saturation intensity in the amplifier (see figure 45a). Laser pulse energies of up to 30 μJ were measured [62]. The laser pulsewidth was measured to be about 0.8ns (see figure 45 b). The corresponding laser intensity at the exit of the plasma column is larger than the computed saturation intensity of 56-78MW/cm^2.

PROSPECTS FOR LASING AT SHORTER WAVELENGTHS

The collisional excitation argon experiment discussed above can, in principle, be scaled in Z along the neon isoelectronic sequence to demonstrate lasing in a discharge-created plasma at shorter wavelengths. Colorado State University researchers have already reported the observation of emission from the J=0-1 of CaXI, and possibly of the equivalent line in TiXIII, in capillary discharge plasmas created by discharge ablation of capillaries containing CaH_2 and TiH_2. Rapid excitation of 1.5 and 2.5 mm diameter capillaries made out of these materials with current pulses of less than 70 kA have produced Ca and Ti plasmas in which atoms are ionized up to the O-like and F -like ions, respectively.

To obtain lasing at wavelengths below 30 nm using the Ne-like sequence, excitation of higher-Z ions, such as Ne-like Cr (λ=28.5 nm) and Ne-like Fe (λ=25.5nm) is required. It is foreseeable that scaling of the excitation to achieve 50-100 μm diameter plasma columns with electron densities near 2-5x10^{20} cm^{-3} and electron temperatures in the range of 500-700 eV, could result in lasing below 20 nm in Ne-like Kr, with gains of the order of 5-8 cm^{-1}. However, those plasma parameters require a significant increase

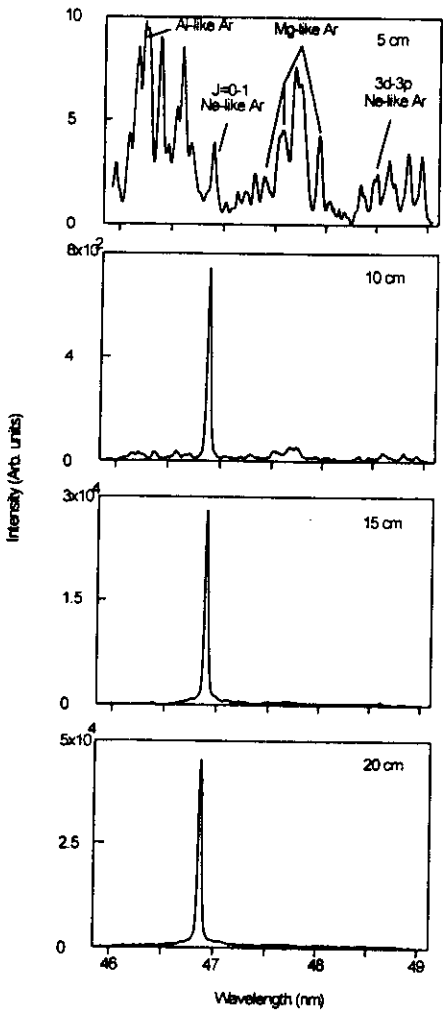

FIGURE 44. Spectra from the capillary discharge argon plasma showing the dramatic increase on the intensity of the 46.9 nm laser line as a function of plasma column length. The spectra correspond to a 4-mm-diameter capillary filled with approximately 720 mTorr of argon, excited by a 39 kA current pulse of 72 ns first half-cycle duration.

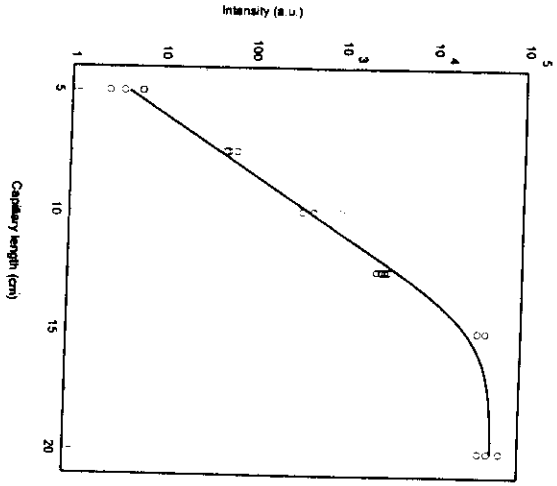

FIGURE 45. Integrated line intensity of the 46.9 nm line of ArIX as a function of plasma column length. The capillary diameter is 4 mm and the argon pressure is ~ 720 mTorr. The maximum gl value reached is 14.1 or 13.4, depending on two slightly different measurements of the attenuation of the filters used. The corresponding gain coefficients for lengths <15 cm determined by the Linford formula are 0.94 cm^{-1} and 0.89 cm^{-1}, respectively. Ref. 23

in the discharge current and voltage. Alternatively, a more rapid scaling to shorter wavelengths could be achieved utilizing Ni-like ions[13,14]. In this case, amplification at wavelengths below 200 Å can be explored, for example, utilizing the $3d^9\,4d\,^1S$ - $3d^9\,4p\,^1P$ transition of MoXIV (λ=18.92 nm). This transition has already been identified in a laser-created plasma, and gain has been measured in the equivalent line in Ni-like Nb (λ=20.42 nm) in a plasma created by a table-top laser[14]. Excitation of these Ni-like transitions in a fast compressive capillary discharge should still require modest currents, of the order of less than 100 kA. It is also possible that scaling of the excitation to generate plasma columns with electron densities near 2-5x10^{20} cm^{-3} and electron temperatures of about 450 eV could produce amplification with gain in the range of 4-6 cm^{-1} in Ni-like Xe in the vicinity of 9.0 nm.

DISCHARGE PUMPED RECOMBINATION LASERS.

Attention has also been devoted to the demonstration of gain by plasma recombination in a capillary discharge. A few groups have in the past few years reported the observation of gain [54,55] and anomously intense emission [56] in the 182 Å (3-2) line of H-like carbon in capillary discharge plasma, a discharge pumping scheme proposed in 1988 [45]. In small diameter capillaries electron heat conduction is expected to contribute to the plasma cooling. In the case of experiments conducted at Ruhr University , in which a short duration spike emission was reported at 18.2nm in polyacetal capillaries, the observed intense spikes were attributed to charge transfer caused by fast ions produced by instabilities [57]. Line enhancement has also been observed in the 4f-3d lines of Li-like ions in a gas liner pinch Kunze [57]. In all experiments to date however the reported laser line intensities remain of the order of non amplified lines (see figure 47), and further work is needed to demonstrate large gain length products in discharge pumped recombination lasers.

spike emission was reported at 18.2nm in polyacetal capillaries, the observed intense spikes were attributed to charge transfer caused by fast ions produced by instabilities [57]. Line enhancement has also been observed in the 4f-3d lines of Li-like ions in a gas liner pinch Kunze [57]. In all experiments to date however the reported laser line intensities remain of the order of non amplified lines (see figure 47), and further work is needed to demonstrate large gain length products in discharge pumped recombination lasers.

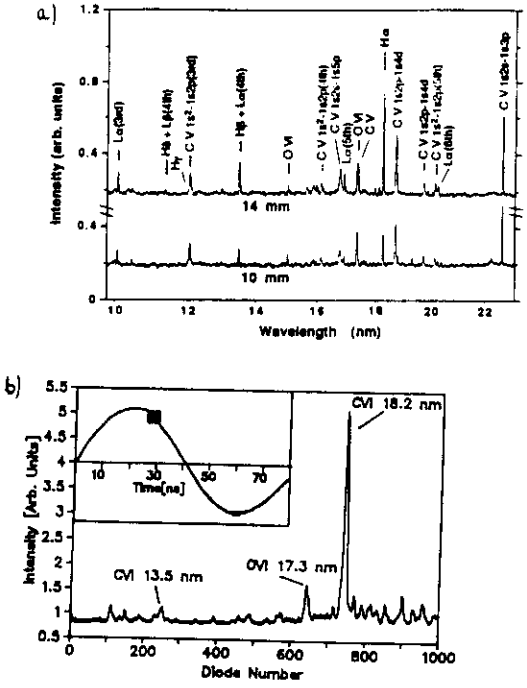

Figure 47 - a) Time integrated spectra obtained using capillary lengths of 14 and 10mm. Each spectra was obtained in Polyethylene capillaries 1.2mm diameter. From ref 55. b) On-axis time resolved spectra of the plasma of a 1mm diameter polyethylene capillary discharge excited by a fast current pulse. From ref 56.

REFERENCES

1) Matthews, P. L. Hagelstein, M. D. Rosen, M. J. Eckart, N. M. Ceglio, A. N. Hazi, M. Medecki, B. J. MacGowan, J. E. Trebes, B. L. Whitten, E. M. Campbell, C. W. Hatcher, A. M. Hawryluk, R. L. Kaufman, L. P. Pleasance, G. Rambach, J. H. Scofield, G. Stone, and T. A. Weaver, "Demonstration of a soft X-ray amplifier," *Phys. Rev. Lett.* **54**, p. 1101 (1985).

2) S. Suckewer, C. H. Skinner, H. Milchberg, C. Keane, and D.Voorhees,"Amplification of stimulated soft X-ray emission in a confined plasma column," *Phys. Rev. Lett.* **55**, p. 1753, (1985).

3) R. C. Elton, "*X-Ray Lasers*," Academic Press, 1990

4) G. J. Lindford, E.R. Peressini, W. R. Sooy, and M. L. Spaeth, "Very long lasers," *Appl. Opt.* **13**, p. 379, (1974).

5) See for example, J. T. Verdeyen, in *Laser Electronics*, Prentice-Hall Series in Solid State Electronics, 1989.

6) S. Suckewer, C. H. Skinner, D. Kim, E. Valeo, D. Voorhees, and A. Wouters, "Divergence Measurements of Soft- X-Ray Laser Beam," *Phys. Rev. Lett.* **57**, p. 1004, 1986.

7) J. J. Rocca, V.N. Shlyaptsev, F. G. Tomasel, O. D. Cortazar, H. Hartshorn, and J. L. A. Chilla, "Demonstration of a discharge pumped table top soft X-ray laser", *Phys. Rev. Lett.* p. **73**, 2192 (1994).

8) H. Fiedorowiexz, A. Bartnik, Y. Li, P.Lu, and E. Fill, "Demonstration of Soft X-Ray lasing with Neon-like Argon and Nickel-like Xenon Ions using a laser irradiated gass puff target", Phys.Rev.Lett. **76**, 415, (1996).

9) B. J. MacGowan, L. B. DaSilva, and D. J. Fields, "Short wavelength X-ray laser research at the Lawrence Livermore National Laboratory," *Phys. Fluids B*, **4**, p. 2326, (1992).

10) A. Carillon, H. Z. Chen, P. Dhez, L. Dwivedi, J. Jacoby, P. Jaegle, G. Jamelot, J. Zhang, M. H. Key, A. Kidd, A. Klishnick, R. Kodama, J. Krishnan, C. L. S. Lewis, D. Neely, P. Norreys, D. O'Neill, G. J. Pert, S. A. Ramsden, J. P. Raucourt, G. J. Tallents, and J. Uhomoibhi, "Saturated and near-diffraction limited operation of an XUV laser at 23.6nm," *Phys. Rev. Lett.* **68**, p 2917, (1992).

11) S. Wang, G. Zhou, G. Zhang, and S. Chunyu, "Overview of research on Ne-like Ge soft X-ray laser in China," in AIP Conf. Proc. 332, X-ray Lasers 1994, Fourth Int. Colloquium, Williamsburg, VA, D. Eden and D. Matthews, Eds., pp. 293-300, 1994.

12) Lewis, D. Nicely, D. M. O'Neil, J. Ouhomoibhi, M. H. Key, Y. Al Hadithi, G. J. Tallents, and S. A. Ramsden, "An injection/amplifier double target configuration for the Ne-like Ge X-ray laser scheme," *Opt. Comm.*, **91**, p. 71, 1992.

13) B.J. McGowan, S. Maxon, L.A. Da Silva, D.J. Field, C.J. Keane, D.L. Matthews, A.L. Osterheld,

14) B. Lemoff, G. Y. Yin, C. L. Gordon III, C. P. J. and S. E. Harris, "Demonstration of a 10 Hz, femtosecond pulse driven XUV laser at 41.8 nm in XeIX," *Phys. Rev. Lett.*, **74**, p. 1574, 1995.

15) P. V. Nickles, M. Schnvrer, M. P. Kalashnikov, I. Will, W. Sandner and J. N. Shlyaptsev, "An efficient short pulse XUV Laser on Ne-like titanium," in **Soft** *X-Ray Lasers and Applications*," Ed. J. J. Rocca and P. L. Hagelstein, SPIE, **2050**, 1995.

16) J. J. Rocca, F. G. Tomasel, M. C. Marconi, V. N. Shlyvaptsev, J. L. Chilla, B. T. Szapiro, and G. Giudice, "Discharge-pumped soft X-ray laser in neon-like argon," *Phys. Plasmas*, **2**, pp. 2547-2554, 1995.

17) V. A. Chirkov, and J. Sov, *Quantum Electron*, **14**, p.1477, 1984.

18) R. A. London, "Beam Optics of Exploding Foil Plasma X-ray lasers," *Phys. Fluids*, **31**, pp. 184-192, 1988.

19) J. L. A. Chilla and J. J. Rocca, "Beam Optics of Gain Guides Soft X-ray lasers," to be published.

20) V. V. Sobelev, *Soc. Astron. AJ* !, p. 665, (1957).

21) G. J. Pert, *J. Phys.* **B 9**, p. 3301 (1976).

22) R. A. London, "Line Escape Probabilities for Exploding Foils," in *Laser Program Annual Report 86*, M. L. Rufer and P. W. Murphy, eds., Univ. Of California report No. UCRL-50021-86 (Lawrence Livermore National Lab, Livermore, California, 1988).

23) J. J. Rocca, M. C. Marconi, J. L. A. Chilla, D. P. Clark, F. G. Tomasel, and V. N. Shlyvaptsev, *IEEE J. Selected topics in quant. Elect.*, **1**, p. 945, 1995.

24) N. M. Ceglio, D. P. Gaines, D. G. Stearns and A. M. Hawryluk, "Double Pass Amplification of Laser Radiation at 131 Å," *Optics Comm.* **69**, p. 285, 1989.

25) N. M. Ceglio, D. G. Stearns D. P. Gaines, A. M. Hawryluk, and J. E. Trebes, "Multipass Amplification of Soft X-rays in a Laser Cavity," *Opt. Lett.* **13**, p.108 (1988).

26) C. J. Keane, N. M. Ceglio, B. J. MacGowan, D. L. Matthews, D. G. Nilson, J. E. Trebs, and D. A. Whelan, "Soft x-ray laser source development and applications experiments at Lawrence Livermore National Laboratory," *J. Phys. B: Al Mol. Opt. Phys.*, **22**, (1989), pp. 3343-3362. Printed in the U. K.

27) D. L. Matthews and M. D. Rosen , Scientific American, p. 86, December 1988.

28) R. C. Elton, *Appl. Optics* **14**, p. 97, (1975)

29) A. Zherikhin, K, Koshelev, and V. Letokhov, *Sov. J. Quant. Mech.* **6**, p.82, (1976)

30) A. V. Vinagradov and v. Shlyaptsev, *Kvatn. Elektron*, (Moscow) **10**, p. 2325 (1983), Sov. J. Quantum Electron, **13**, p. 1511 (1983).

31) a) T.N. Lee, E.A. McLean and R.C. Elton, "Soft x-ray lasing in Neon-like germanium and copper plasmas", Phys. Rev.Lett. **39**, 1187, (1987) - b) B.J. MacGowan et.al. J.Appl.Phys. **61**, 5243, (1987).
32) J. Nielsen, B.J. MacGowan, L.B. DaSilva, and J.C. Moreno, "Prepulse technique for producing low Z Ne-like x-ray lasers", Phys.Rev.A, **48**, 4682, (1993).
33) J.C. Nielsen, J.C. Moreno, B.J. MacGowan and J.A. Koch, "First observation of lasing at 231Å in Neon like Nickel using the pre-pulse technique", Appl.Phys. B 309, (1993).
34) T. Boehly et. Al., "Demonstration of a Narrow Divergence X-Ray Laser in Neon Like Titanium," *Phys. Rev. A* **42**, p. 6462, 1990.
35) See papers in session "Soft X Ray Lasers Utilizing the Prepulse Technique," in "Soft X-Ray Lasers and Applications," Eds. J. J. Rocca and P. L. Hagelstein, *SPIE*, **2520**, (1995).
36) E. E. Fill, Yuelin Li, G. Pretzler, D. Schlogl, and J. Steingruber, "Investigation of lasing on the J = 0-1 line of neon -like ions using the prepulse technique," "Soft X-Ray Lasers and Applications," *SPIE*, **2520.**
37) B. J. MacGowan, S. Maxom, P. L. Hagelstein, C. J. Keane, R. A. London, D. L. Matthews, M. D. Rosen, j. H. Scofield, and D. A. Whelan, *Phys. Rev. Lett.* **59**, p. 2157. (1987).
38) H. Daido, Y. Kato, K. Murai, S. Ninomiya, G. Yuan, y. Oshikane, M. Takagi, H. Takabe and F. Koike, "Efficient Soft X-Ray Lasing at 6 to 8 nm with Nickel-like Lanthanide Ions," *Phys. Rev. Lett.*, **75**, p. 1074, 1995.
39) N. H. Burnett and P. B. Corkum, *J. Opt. Soc. Am.* **B 6**, 1195 (1989) and P. B. Corkum and N. H. Burnett, in Short-Wavelength Coherent Radiation: Generation and Applications, R. W. Falcone and J. Kirz, eds., Vol. 2 of OSA Proceedings Series (Optical Society of America, Washington, D. C., 1988). p. 225.
40) B. E. Lemoff, C.P.J. Barty, and S. E. Harris, " Femtosecond- pulse driven, electron-excited XUV lasers in eight-times-ionizable noble gases," *Optics Lett.* **19**, p. 569, 1994.
41) L. L. Gudzenko and L. A. Shelepin, *Soc. Phys. Doklady*, **10**, p. 147, (1965).
42) P. Jaegle, G. Jamclot, A. Carillon, A. Klisnick, A. Sureau, and H. Gucnnou, *J. Opt. Soc. Am.* **B 4**, 563 (1987), and G. Jamelot, et. al., *IEEE Trans. Plasma Science*, **16**, p.497 (1988).
43) J. C. Moreno, H. R. Griem, S. Goldsmith and J. Knauer, Phys. Rev. A 39, p. 6033,(1989), and C. H. Skinner, et. al., *SPIE Proceedings 875*, **20** (1988) and *J. Opt. Soc. Am.*, **6**, p. 115 (1989).
44) P. Amendt, D. C. Eder, and S. C. Wilks, *Phys. Rev. Lett.* 66, p. 2589, (1991) and D. C. Eder, P. Amendt, and S. C. Wilks, *Phys. Rev.* A **45**, p. 6761 (1992).

45) Yutaka Nagata, Katsumi Midorikawa, Shoich Kubodera, Minoru Obara, Hideo Tashiro, and Koichi Yoyoda, "Soft-X-Ray Amplification of the Lyman-α Transition by Optical-Field induced Ionization," *Phys. Rev. Lett*, **71**, p. 3774, 1993.
46) S. M. Hooker and S. E. Harris, "Femtosecond-pulse -driven electron-excited extreme-ultraviolet lasers in Be-like ions," *Optics Lett.*, **20**, 1994, (1995).
47) H. M. Milchberg, C.G. Durfee III, and J. Lynch, "Application of a plasma waveguide to soft x-ray lasers', J. Opt.Soc.A, B, 12, 731, (1995).
48) S. Basu, P.L. Hagelstein, J.G. Goodberlet, M.H. Muendel, and S. Kaushik, "Amplification in Ni-like Nb at 204Å pumped by a table-top laser", Appl. Phys. B57, 303, (1993).
49) J. Goodberlet, S. Basu, M.H. Muendel, S. Kaushik, T. Savas, M. Fleury, and P.L. Hagelstein, "Observation of gain in a recombination H-like boron plasma", J.Opt.Soc. Am B **12**, 980, (1995).
50) J. Goodberlet, T. Savas, S. Basu, M. Muemdel, S. Kaushik, M. Fleury, and P. L. Hagelstein, "Recent experiments with the MIT table-top X-ray laser system," *Proceedings of the International Conference on Lasers*," (1994).
51) T. Hara, M. Aoyama, K. Ando and y. Aoyagi, "Compact soft X-Ray Laser Pumped by a Pulse Train," in "X-Ray Lasers and Applications," Eds. J. J. Rocca and Polo Hagelstein, *SPIE*, **2520**, p. 217, 1995.
52) A. Morozov, L. Polonsky, and S. Suckewer, "Towards compact soft x-ray lasers," in "X-ray Lasers and Applications," Eds. J. J. Rocca and P. Hagelstein, *SPIE*, **2520**, p. 180, 1995.
53) R. W. Waynant, *Phys. Rev. Lett.*, **28**, p. 553, 1972.
54) J. J. Rocca, D. C. Beetle and M. C. Marconi, "Proposal for XUV and Soft X-Ray Lasers in a Capillary Discharge," *Opt. Lett.*, **13**, p.565, 1988.
55) J.J. Rocca, O.E. Cortazar, B.T. Szapiro, K. Floyd and F. Tomasel, Phys. Rev. E **47**, 1299, (1993).
56) J. J. Rocca, O. D. Cortazar, F. G. Tomasel and B. T. Szapiro, "Efficient Generation of Highly ionized Calcium and Titanium plasma Columns for Collisionally Excited Soft X-Ray Lasers in a Fast Capillary Discharge," *Phys. Rev.* E., **E 48**, p. 2378, 1993.
57) C. Steden and H. J. Kunze, "Observation of Gain at 118.2 nm in the carbon plasma of a capillary discharge," *Phys. Lett. A*, **151**, p1534, 1990.
58) H.J. Shin, D.E. Kim and T.N. Lee, Phys. Rev. E
59) J. J. Rocca, M. C. Marconi, B. T Szapiro, and J. Meyer, "Experiments on soft X-ray laser development in a table top capillary discharge," in "Ultrashort wavelength lasers," Ed., S. Suckewer, *SPIE*, **1551**, p.275, 1991.

60) H. J. Kunze, S. Glenzer, C. Steden, H. T. Wieschebrink, K. N. Koshelev, and D. Uskov, Lasing at Short Wavelength in a Capillary Discharge and in a Dense Z-Pinch," in *X-Ray Lasers* ,1994, Ed. D. Eder and D. Matthews, *AIP Conference Proc.* **3323**, p.380, 1995.

61) D. Korobkin, C.H. Nam and S. Suckewer. Phys. Rev. Lett, Dec. 1996.

62)J.J. Rocca, D. P. Clark, J.L.A. Chilla and V.N. Schlyaptsev. Phys. Rev. Lett. 1476. 77. (1996).

Applications of Soft X-Ray Lasers

Applications of Soft X-Ray Lasers

Status (Feb. 1997)

Application	No Experiment Performed to date	Proof of Principle Experiments	Advanced Development	References
Holography		X		1
Microscopy				2-4
Diagnostics of Dense Plasmas (Interferometry, Imaging)			X	5-7
X-Ray induced luminescence of crystals (e.g. Scintillator detectors)		X		8
X-Ray Optics Tests		X		
Material Science, Photochemistry and Photophysics, Atomic Physics	X			
Lithography	X	(Unlikely to be competitive with other sources)		
X-Ray Non-Linear Optics	X			

Characteristics of Soft X-Ray Lasers

Present Status (January 1997)

Wavelength	35Å[(a)] - 600Å	[(a)] Ni-line Au laser
Power	40kW[(b)] - 30MW[©]	[(a)] Table-top laser [©] Laboratory size laser
Energy	30μJ[(a)] - ≃ 10mJ[©]	[(a)] Table-top laser [©] Laboratory size laser
Pulse Length	50ps - 10 ns	
Beam Divergence	1.5 - 15 mrad	
Longitudinal Coherence	~100μm	
Spatial Coherence	~100μm effective source size	

Soft X-Ray Laser Characteristics

Beam Divergence (of soft x-ray laser without cavity).

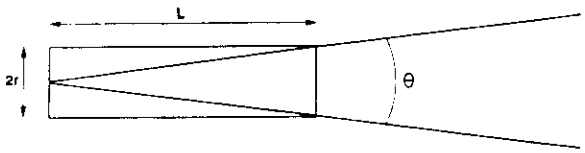

In a first approximation $\theta = \frac{2r}{L}$

For sufficiently large **g x l** the gain distribution forms a waveguide. A Gaussian transverse mode sustained by the waveguide diverges with:

$$\theta = \frac{2\lambda}{\pi \omega_o}$$

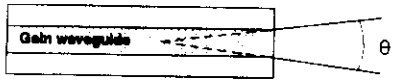

However, in most cases in practice the beam divergence is defined by refraction due to variation of the index of refraction due to radial plasma density gradients in the plasma column.

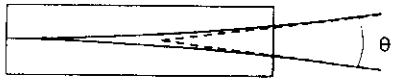

Characteristics of Soft X-Ray Lasers

Intensity

The intensity of the amplified beam increases exponentially until it reaches the saturation intensity I_s, value at which the stimulated emission rate reduces the population inversion and the gain by half.

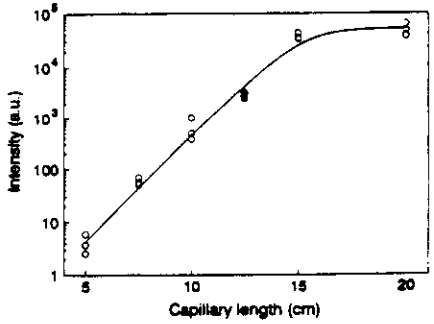

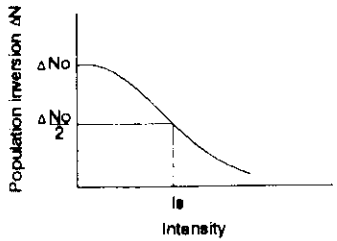

where $g_o = \sigma \Delta N = \frac{A_{21}\,\lambda^2}{8\pi\,\Delta_\nu}(N_2 - N_1\,\frac{g_2}{g_1})$ is the small signal gain.

For an inhomogeneously broadened line:

$$g(z) = \frac{g_o}{\sqrt{1 + \frac{I}{I_s}}}$$ saturated gain

where $I_s = \frac{h\nu}{\sigma\tau}$ saturation intensity.

τ is the effective lifetime of the laser upper level.

In soft x-ray lasers normally $\tau \gg \frac{1}{A_{21}}$ due to collisional electron excitation

of the laser upper.

Typically: $\frac{A_{21}}{\tau} = 20\text{-}200$

For example for a Ne-like Y laser:

$\lambda = 15.5$ nm

$A_{21} = 1.3\ 10^{10}\ s^{-1}$

$\tau^{-1} = 2.2\ 10^{12}\ s^{-1}$

$K_{ti} = 0.6$ KeV

Laser output pulsewidth ~ 200 ps

$$I_s = \frac{8\pi\sqrt{\pi}\ h\nu^3\Delta\nu}{c^2}\ \frac{1}{\tau A} \sim 1\ 10^{11}\ W/cm^2$$

Output Power

The laser power will be a few times larger than $P = I_s\ \pi\ r^2$

For the Y laser with $2r = 100\ \mu m$ ➡ $P = 8\ 10^6$ W.

30 MW have been measured by L. Da Silva et al., Optics. Lett., 1174, **18,** (1993).

Focusing of this beam to a realistic spot of ~ 1μm ϕ with a Schwarzchild microscope objective should give:

$$\text{Power Density} \sim \frac{8\ 10^6\ W}{8\ 10^{-9}\ cm^2} = 1\ 10^{15}\ W/cm^2$$

Sufficient intensity for non-linear optics experiments.

Moreover, if a diffraction limited beam could be obtained extremely high power densities could be obtained focusing the beam

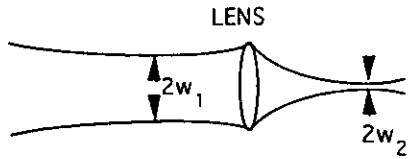

$$W_2 = \frac{F\lambda}{\pi w_1} \sim \frac{\lambda}{\pi N_A}$$

where N_A is the numeral aperture of the following optics (most likely reflective optics).

For NA = 0.5, and for the example above:

$W_2 \sim 1.5\ 10^{-8}$ m
and Power Density ~ 10^{22} W/cm^2

A diffraction limited soft x-ray laser however has not yet been achieved.

Brightness of Soft X-Ray Sources

If the beam divergence is determined by the geometry of the amplifier, the saturated brightness is:

$$B_S \sim I_s \left(\frac{L}{d}\right) \text{ W cm}^{-2} \text{ sterad}^{-1}$$

From the previous example $I_s \approx 1\ 10^{11}$ W/cm^2 and for d ≈ 100μm = 0.01 cm and L = 5cm ➡ $B_s \approx 2.5\ 10^{16}$ W cm^{-2} sterad^{-1}.

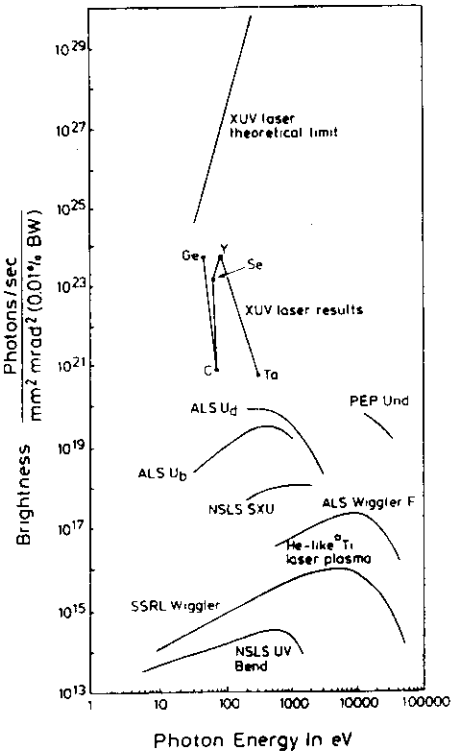

Plot taken from M. Key in "Applications of X-Ray Lasers," Proc. of Workshop, Edited by R. London, D. Matthews and S. Suckewer, San Francisco, 1992.

Characteristics of Soft X-Ray Lasers

Linewidth and Temporal Coherence

The longitudinal coherence is related to the linewidth $\Delta\nu$ by:

$$L_{fc} = \frac{c}{2\Delta\nu} = \frac{\lambda^2}{2\Delta\lambda}$$

The linewidth $\Delta\nu$ of the laser transition in soft x-ray lasers is usually dominated by Doppler broadening.

$$\Delta\nu_D \approx \frac{2.210^4}{\lambda}\sqrt{\frac{Ti}{M}}$$

T, ion temperature in °K

M: mass in AMU

and $\frac{\Delta\lambda}{\lambda} = 7.710^{-5}\sqrt{\frac{T_i}{M}}$ T_i in eV, M in AMU

Typical Linewidths of Soft X-Ray Laser Transitions

λ(nm)	Specie	T_i(eV)	M	Δλ/λ
15.5	Ne-like y	600	89	$2\ 10^4$
46.9	Ne-like Ar	70	40	$1.2\ 10^4$

Gain Narrowing

The linewidth of the laser line is narrowed due to amplification by

$\approx \frac{1}{\sqrt{g\ell}}$. For a saturated soft x-ray laser $g \times \ell \approx 16\text{-}20$ consequently:

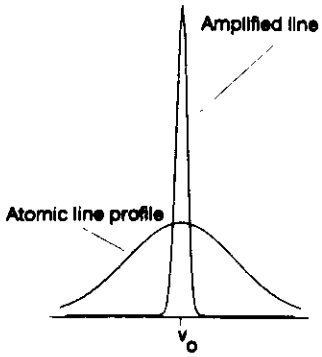

$$\frac{\Delta\lambda}{\lambda}\Big|_{laser} \approx \frac{\Delta\lambda}{\lambda}\ \frac{1}{\sqrt{g\ell}} \approx 5 \times 10^{-5}$$

Saturation effects can contribute to re-broaden the line, depending on the line profile.

$$\text{For } \lambda = 200\text{Å} \text{ and } \frac{\Delta\lambda}{\lambda} = 5 \times 10^{-5} \rightarrow L_{tc} = 150\mu m$$

Characteristics of Soft X-Ray Lasers

Spatial Coherence

Spatial (or transverse) coherence relates to different spatial portions of the beam interfering with each other. Assuming a homogeneous amplifier the transverse coherence length is given by:

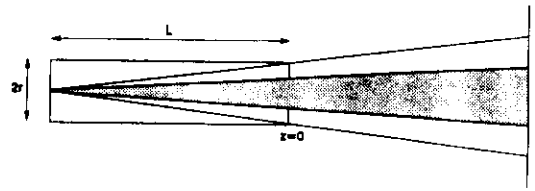

$$l_{TC} = \frac{\lambda L}{2\pi r} = \frac{r}{2\pi N}$$

where $N = \frac{r^2}{\lambda L}$ is the Fresnel number. The beam at the exit of the amplifier is

fully coherent if $l_{TC} = 2r$

For example for a Ne-line Ge soft x-ray laser[1]:

$\lambda = 234A$ $\quad L = 5cm$ $\quad 2r = 50\mu m$ $\quad N=0.53$

$$l_{TC}(z) \approx 7.5\ \mu m$$

The transverse coherence length of radiation at an observation plane at a

$$l_{TC}(z) = [l_{TC}^2(0) + (\frac{\lambda z}{2\pi r})^2]^{1/2}$$

distance z from the radiation source is

(1) Y. Kato et al., p. 56, SPIE Vol. 1551, 1991.

when z >> L the second term is dominant and the spatial coherence is dominated by the source size.

At 100 cm from the source, for the above Ne-like Ge laser example:

$$\ell_{TC}(z) \approx \frac{\lambda z}{2\pi r} \approx 150\mu m$$

If the optical medium of the laser is spatially inhomogeneous, this introduces distortion of the wave front changing the spatial coherence.

Measurement of the Coherence of An X-ray Laser Using a Mach-Zehnder Interferometer

(Experiment performed with a Ne-line Y laser, $\lambda = 15.5$ mm)*

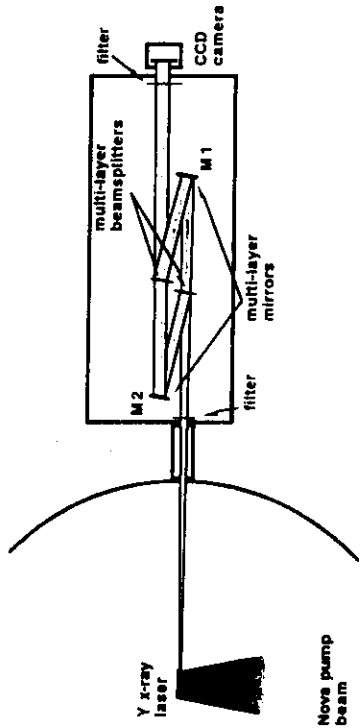

To measure the temporal coherence the mirror M_1 was translated to vary the path length difference of the two interferometer arms

*L.B. Da Silva et al. (Lawrence Livermore Laboratory).

Measurement of the Coherence of an X-Ray Laser Using a Mach-Zehnder Interferometer

Temporal (longitudinal) coherence

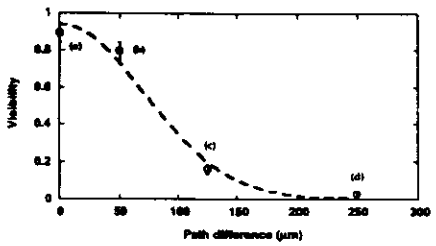

where fringe visibility $V = (I_{MAX} - I_{MIN})/(I_{max} + I_{min})$
The fringe visibility is the envelope of the autocorrelation function for the power spectrum, which varies with path difference c according to

$V(\tau) = \exp[-\pi\Delta\nu\tau/(2\sqrt{\ln_2})^2]$
where a Gaussian lineshape was assumed.

A Gaussian fit to the measured fringe visibility yielded a 1/e half-width of c ~ 100μm

(Equivalent Gaussian FWHM linewidth 13mÅ)

Spatial Coherence
(From spatial decay of fringe visibility)

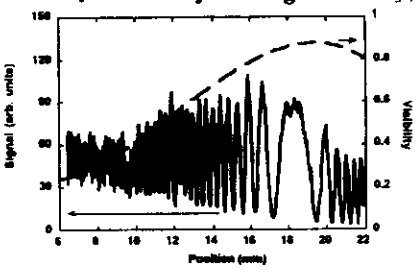

The fringe visibility was fitted with

$$V(\Delta X) \approx \exp[-(\frac{\Delta X}{a})^2]$$

with a = 0.16, which yields an effective source diameter

$$a = \theta tz(z) = \frac{\lambda z}{r} \rightarrow r \approx 220\mu m$$

with a 50% error.

Finite temporal coherence: fringe contrast varies with path length difference

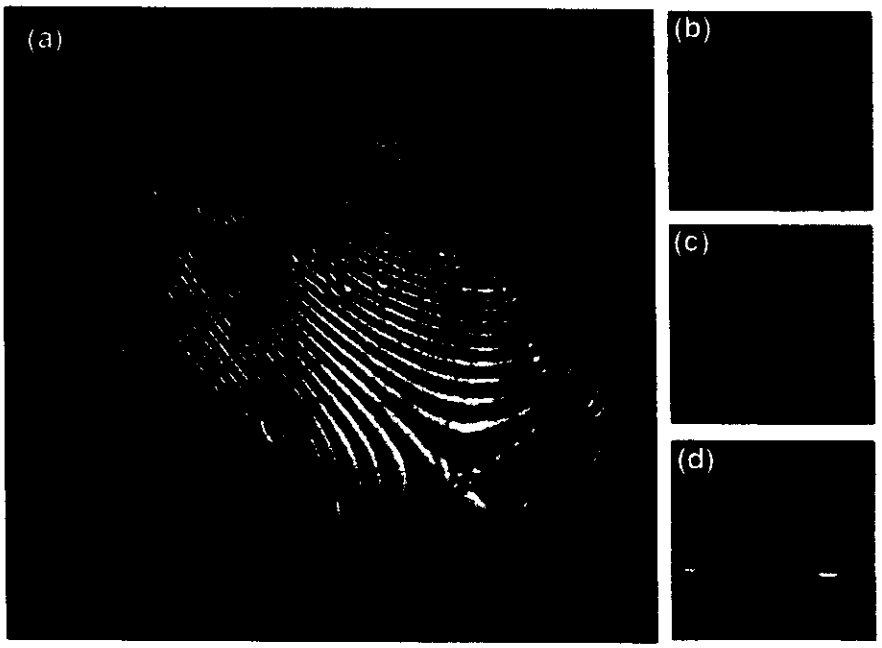

(a) 0 μm; (b) 50 μm; (c) 125 μm; (d) 250 μm

Examples of Applications of Soft X-ray Lasers Already Realized in the Laboratory

- Soft x-ray imaging; soft x-ray microscopy.
- Soft x-ray holography.
- Diagnostics of high density plasma: Interferometry and Imaging.
- Soft x-ray laser excited luminescence of ionic crystals.

Test of Soft X-Ray Contrast Microscopy

(Using 18.2 CVI Recombination Laser*)

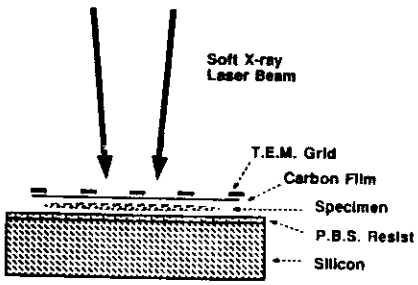

SEM image of replica of hela cells (Helen Lane cervical cancer cell). 0.1 μm resolution.

*D.S. Di Cicco et al. "Contact Microscopy With a Soft X-Ray Laser", p. 277 in OSA Proc. "On Short Wavelength Coherent Radiation Generation and Applications," Ed. R. Falcone and J. Kirz, 1988.

X-ray imaging with the Ta x-ray laser has achieved diffraction limited resolutions of 500 Å.

Test pattern imaged with 200 ps Ta x-ray laser

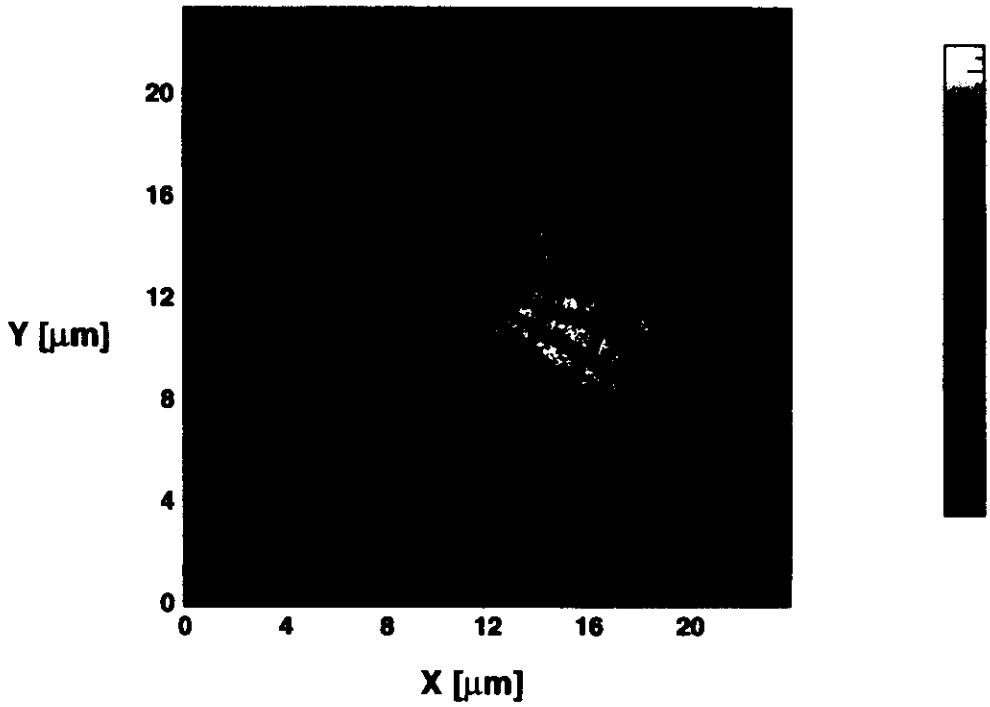

The use of gold labeling can significantly enhance contrast in x-ray images

- **Gold labeling reduces the required incident flux and allows the location of selected proteins to be mapped out**

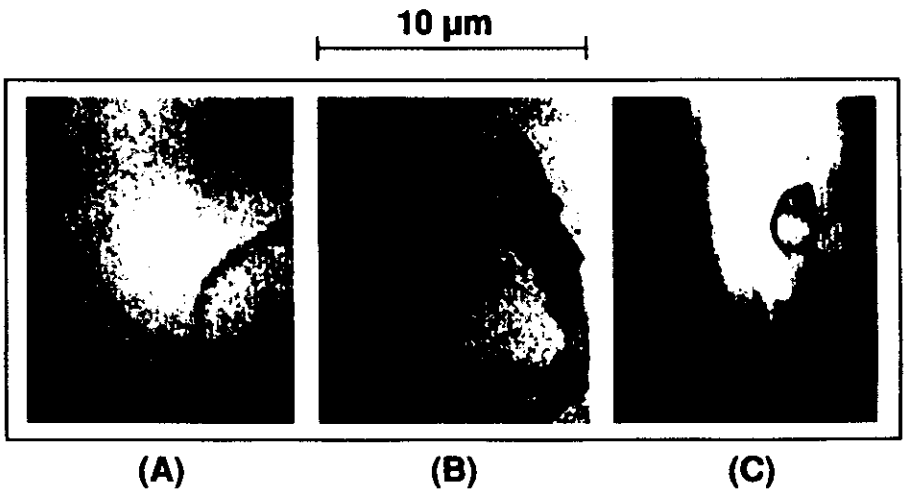

Test of Soft X-Ray Holography

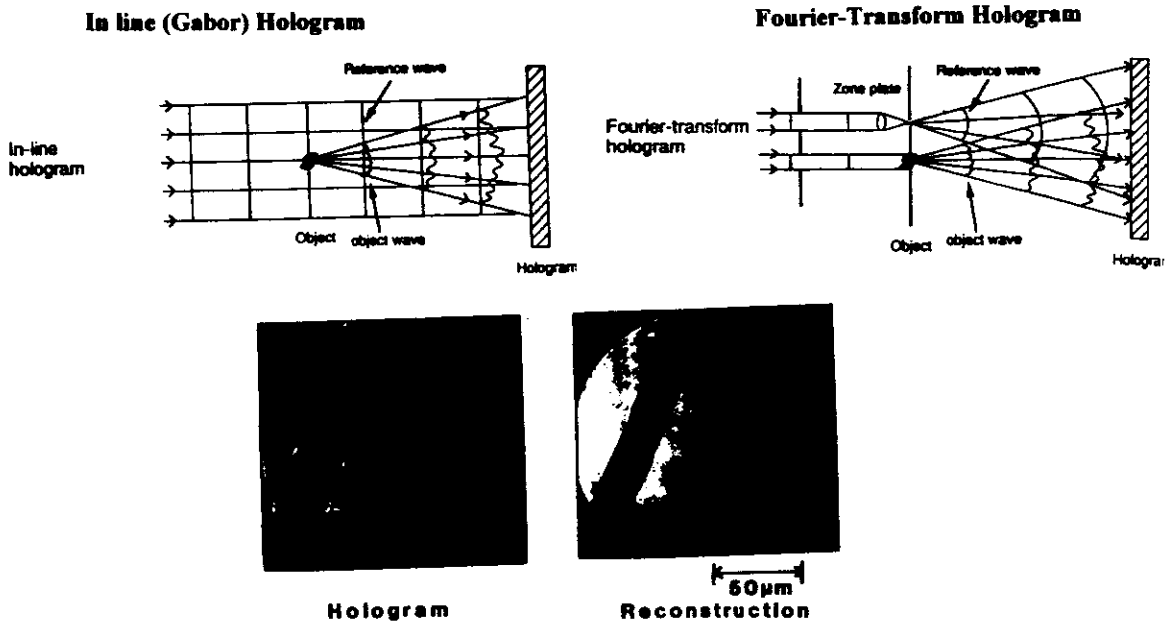

In line hologram of an electron microscope test pattern (left) and it's numerical reconstruction (right). Recorded on PMMA Photoresist, Ref: Y. Kato et al. SPIE, Vol. 2012, p. 12, (1993).

Laser Probing of High Density Plasmas

Limitations		Solution
1. Plasma Absorption (Limits Maximum ne*L)	→	Short Wavelength
2. Refraction (Limits Maximum ne*L)	→	Short Wavelength
3. Rapid Changes in Plasma Density (Limits Maximum Exposure Time)	→	Short Pulse
4. Bright Plasma Radiation (Makes probe hard to detect)	→	High Brightness

Limitations in Laser Probing of High Density Plasma

1. Absorption of the Laser Probe Radiation

In a plasma dominated by Free Absorption the absorption coefficient is:

$$\alpha \approx 2.44\ 10^{-37}\ \frac{\langle Z^2 \rangle\ ne\ ni}{\sqrt{KT(h\nu)^3}} \left[1 - \exp\left(\frac{-h\nu}{KT}\right)\right] cm^{-1}$$

where: KT electron temperature in ev
hν photon energy in ev
ne electron density in cm^{-3}
Ni ion density in cm^{-3}
Z = ion charge

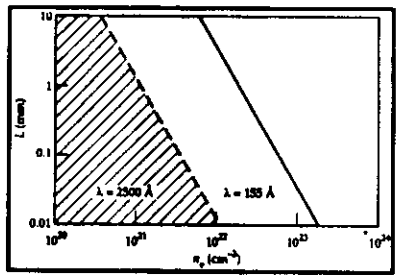

Parameter space accessible for plasma probing . Only free-free absorption is considered

For example for λ = 155Å (Ne-like Y laser)

$Z \approx 30$, KT = 1 Kev

$\alpha = 2.6 \times 10^{-43}\ n_e^2$

For one optical depth (i.e., αL = 1) $n_e^2 L = 3.8\ 10^{42}$

- Resonant line absorption is possible but unlikely given the narrow bandwidth of the x-ray laser ~10mÅ.

Figure from L.B. Da Silva, SPIE, Vol. 2520, P. 289, 1995.

Limitations in Laser Probing of Higher Density Pressure

2. Refraction

Deflection angles imply significant spatial blurring and reduced spatial resolution.

For a with a linear density gradient $n_e = n_o \left(1 - \frac{y}{y_o}\right)$

The deflection angle, θ, scales as: $\theta\ \alpha\ \frac{\lambda^2 L}{y_o}$

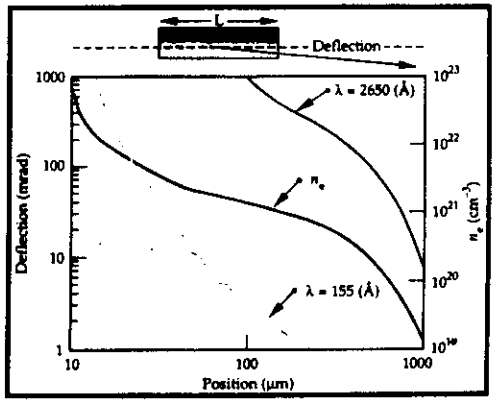

Calculated density and deflection for an optical and an x-ray laser probe traversing 3 mm of plasma created by driving a 50-μm thick CH target with a 1-ns square 0.53 μm lsaer pulse at 2.0×10^{13} W/cm^2.

Adverse refraction effects can be significantly reduced bythe use of a short wavelength probe.

Figure from L.B. Da Silva, SPIE, Vol. 2520, P. 289, 1995.

3. Detector Resolution

In addition to absorption and refraction the maximum ne*L is limited by the detector resolution. The maximum number of fringe shifts:

$$N_{FS} \approx \frac{n_e L}{2 n_c \lambda} \leq 50$$

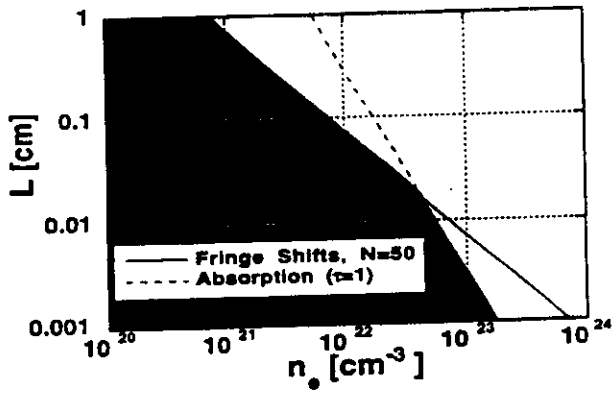

Shaded area is accessible parameter space of electron density and plasma size (L) constrained by absorption (assuming only free-free, T_e=1 keV, <Z>=30. λ=155 Å)

Figure from L.B. Da Silva, SPIE. Vol. 2520, P. 289, 1995.

Plasma Imaging Using a Laser Backlighter *

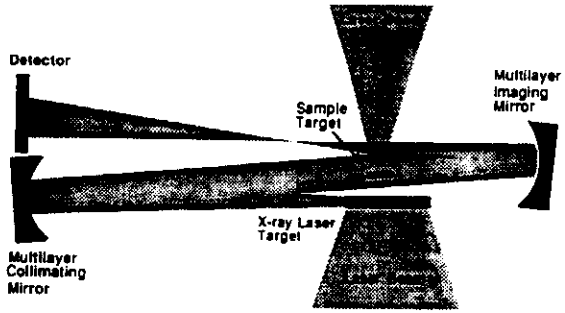

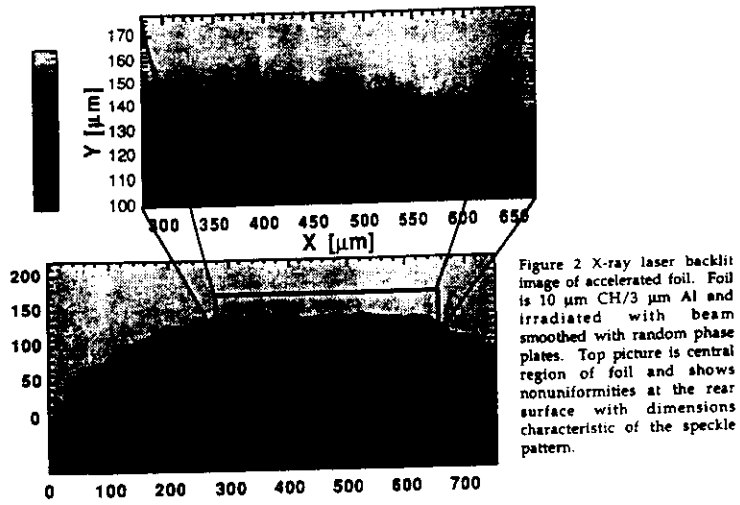

Figure 2 X-ray laser backlit image of accelerated foil. Foil is 10 μm CH/3 μm Al and irradiated with beam smoothed with random phase plates. Top picture is central region of foil and shows nonuniformities at the rear surface with dimensions characteristic of the speckle pattern.

*L.B. Da Silva et al., SPIE Vol 2012, P. 158, 1993.

Soft X-Ray Laser Interferometry of High Density Plasmas

Time Resolved Maps of Electron Density in a Plasma Can be Obtained by Laser Interferometry.

Mach-Zehnder Interferometer

CCD Detector

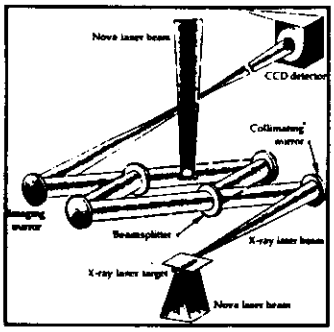

Number of fringe shifts caused by difference in optical path length:

$$N_{FS} = \frac{\delta\phi}{2\pi} = \frac{1}{\lambda}\int_0^L (1-\eta_r)dL \approx \frac{n_e\, L}{2\eta_{cr}\lambda}$$

The index of refraction η_r is related to the electron density η_c by:

$$\eta_r = \sqrt{1 - \frac{n_e}{n_c}}$$

Where the critical density $n_c = 1.1 \times 10^{21}\ \lambda^{-2}\ [cm^{-3}]$ (λ in μm)

Without Plasma With Plasma

Experimental setup used for xuv interferometry of laser produced plasma

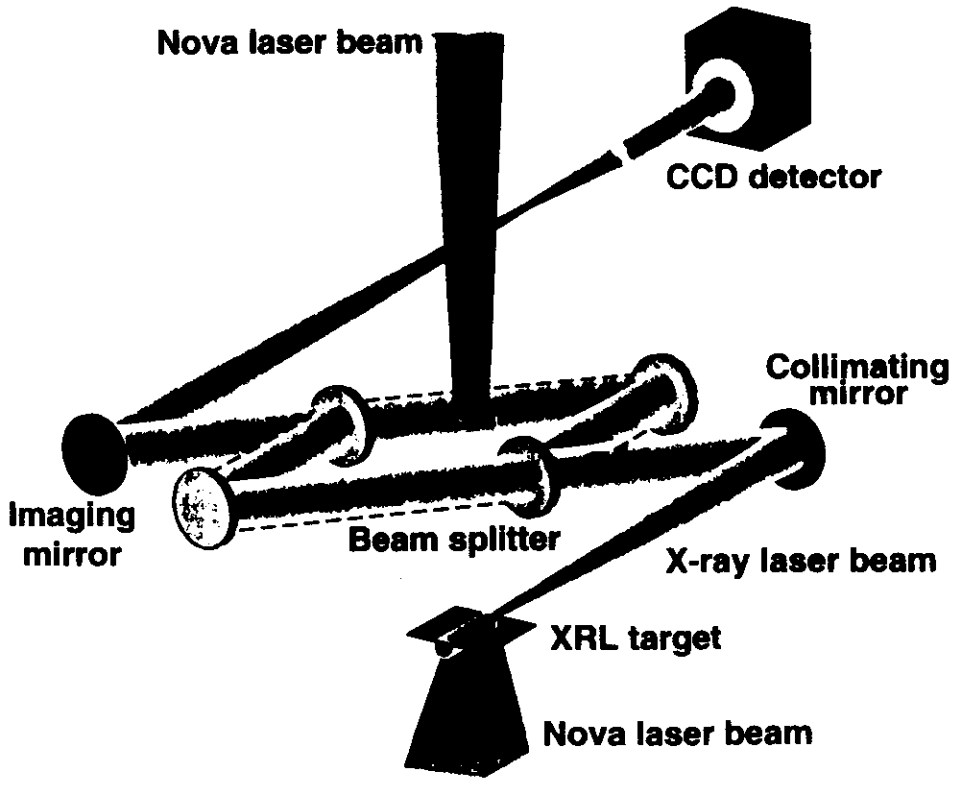

Interferogram obtained without a plasma shows excellent fringe visibility and flatness

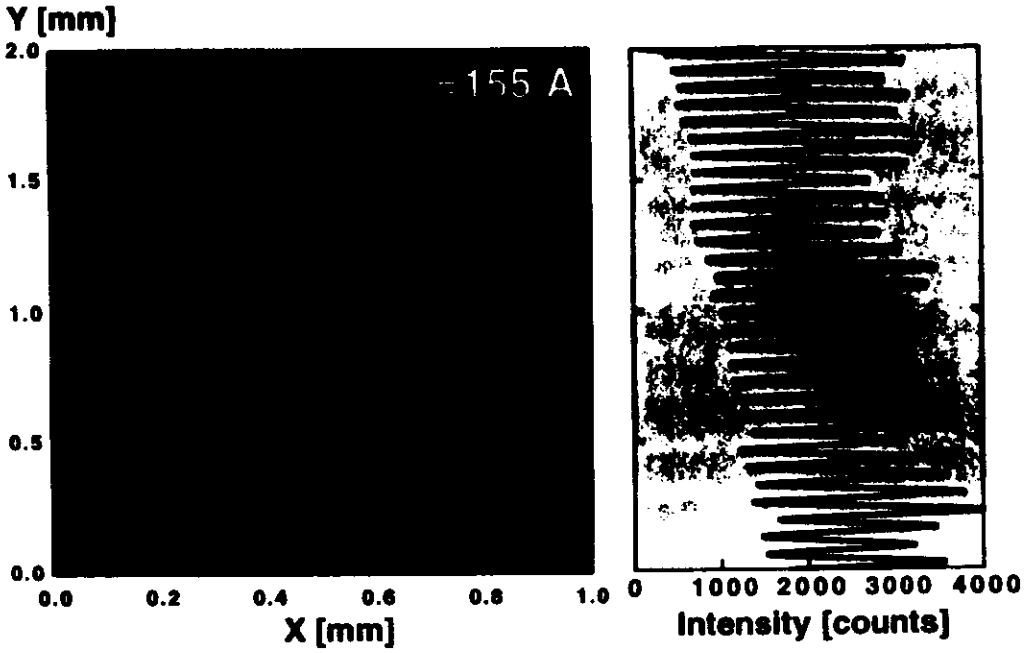

Fringe Visibility varies form 85% to 40% over field of view

Xuv interferogram of laser irradiated CH target obtained with 155 Å soft x-ray laser

CH Target irradiated at 2.7×10^{13} W/cm² with 0.53 μm laser light and backlit 1.1 ns after start of drive

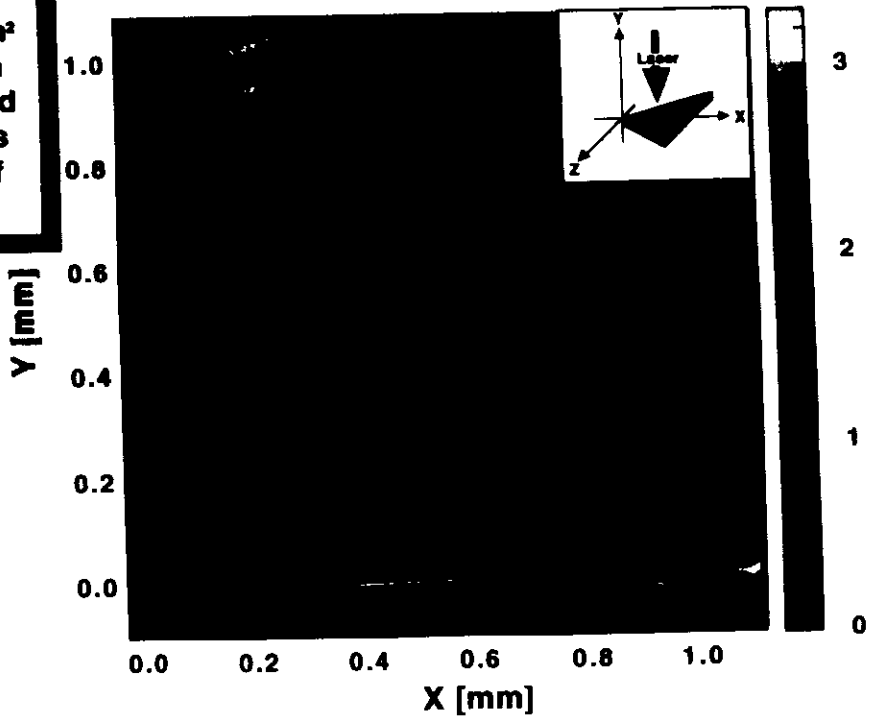

Colliding plasma interferogram shows clear evidence of interpenetrating plasmas

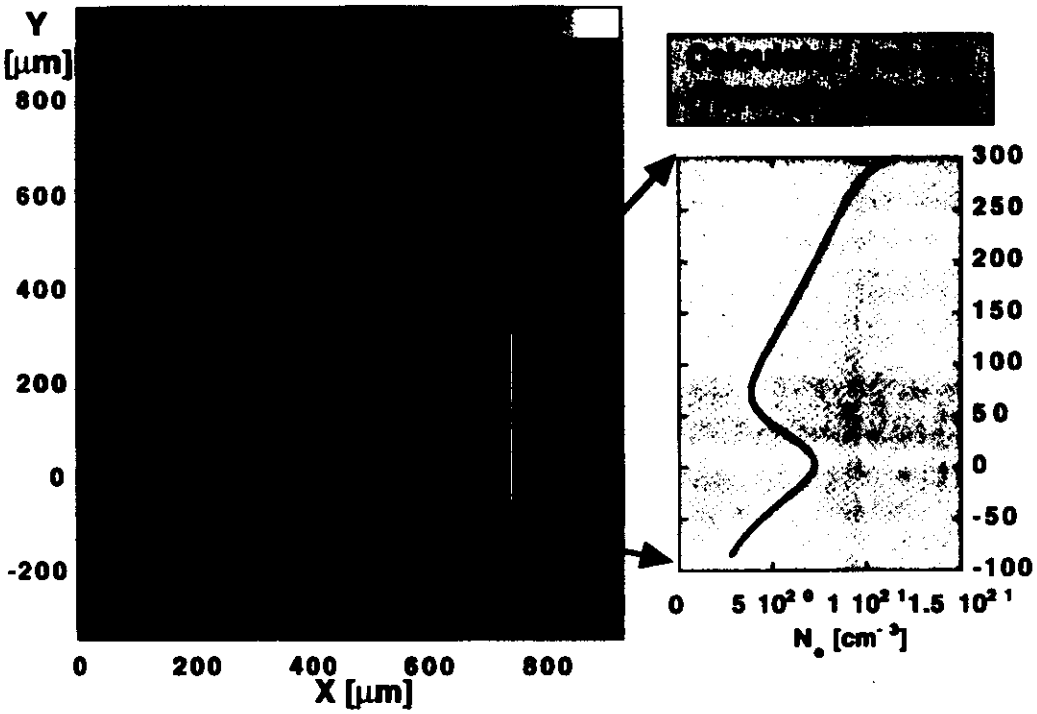

For details, see talk A. Wan 8E.09

Temporal evolution of Se exploding foils was measured with multiple shots

Exploding foil consisting of 800 Å of selenium coated on 1000 Å of lexan, irradiated at 8×10^{13} W/cm^2

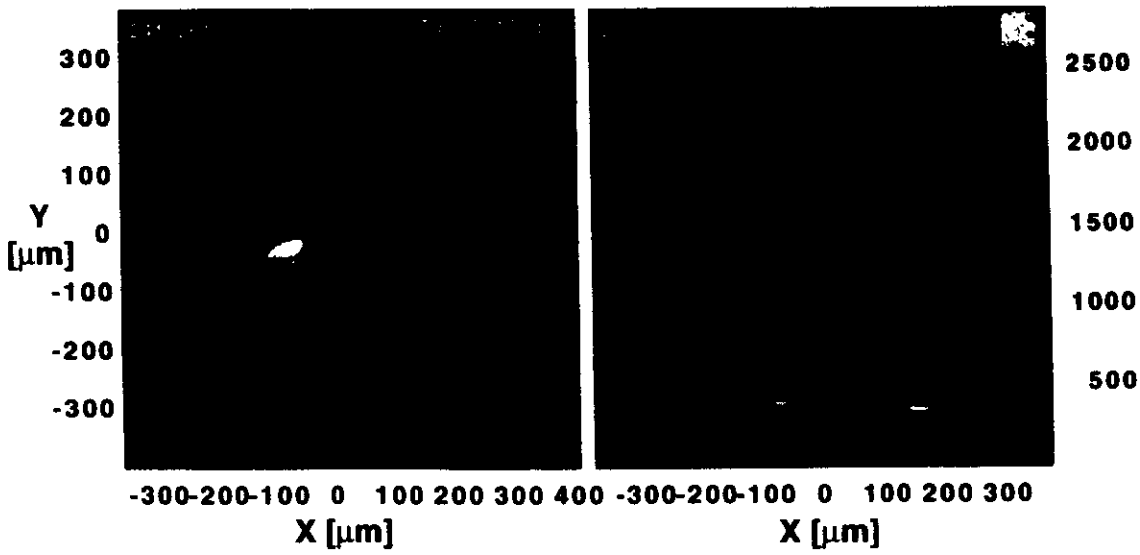

X-ray laser interferogram (λ=21.2 nm, 1 shot)

(Fresnel interferometer)

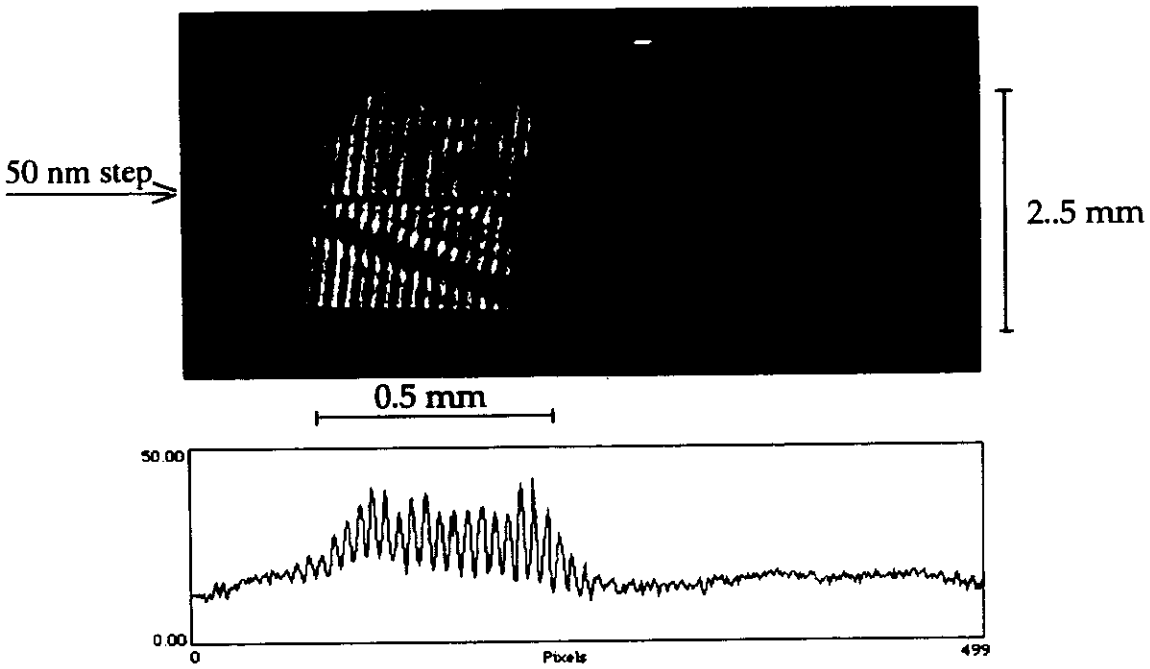

LSAI-IOTA-LULI

Interferometry experiment

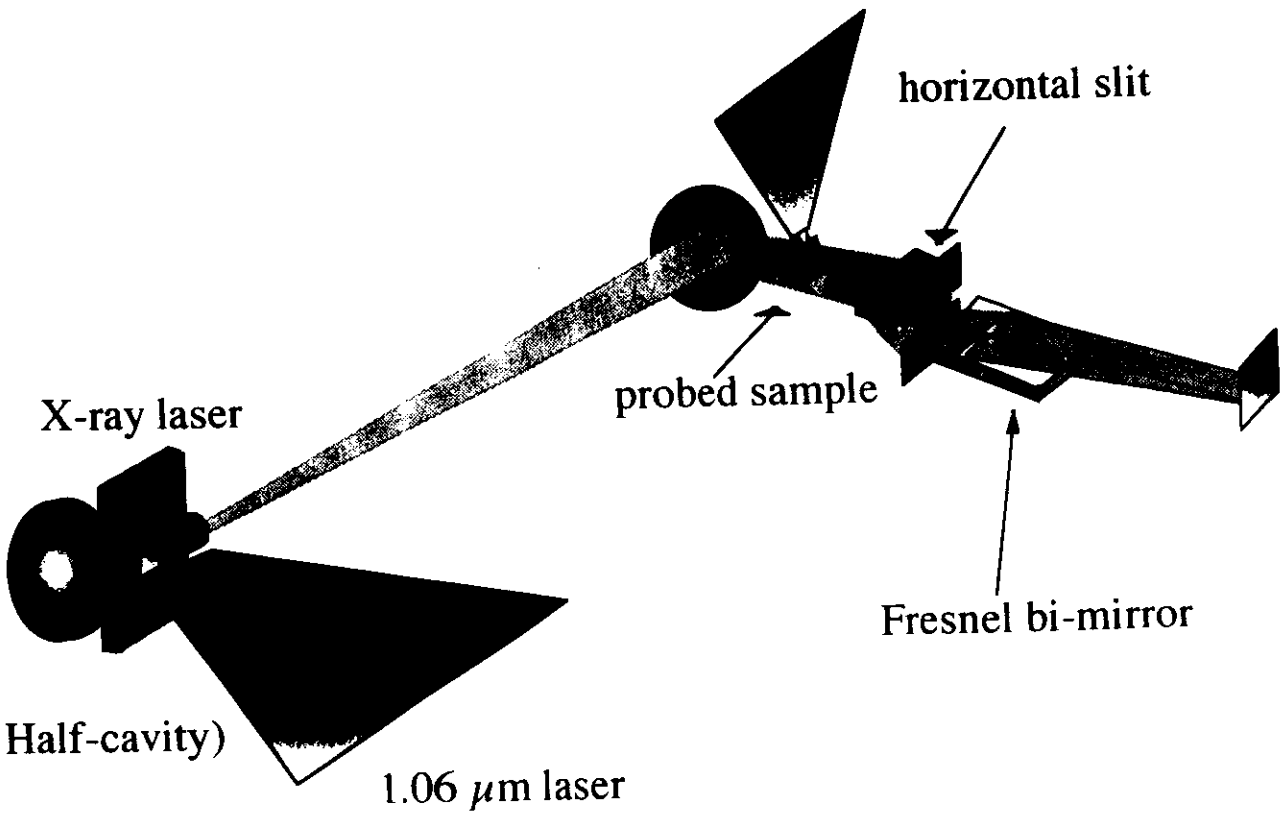

X-ray laser excited luminescence investigation

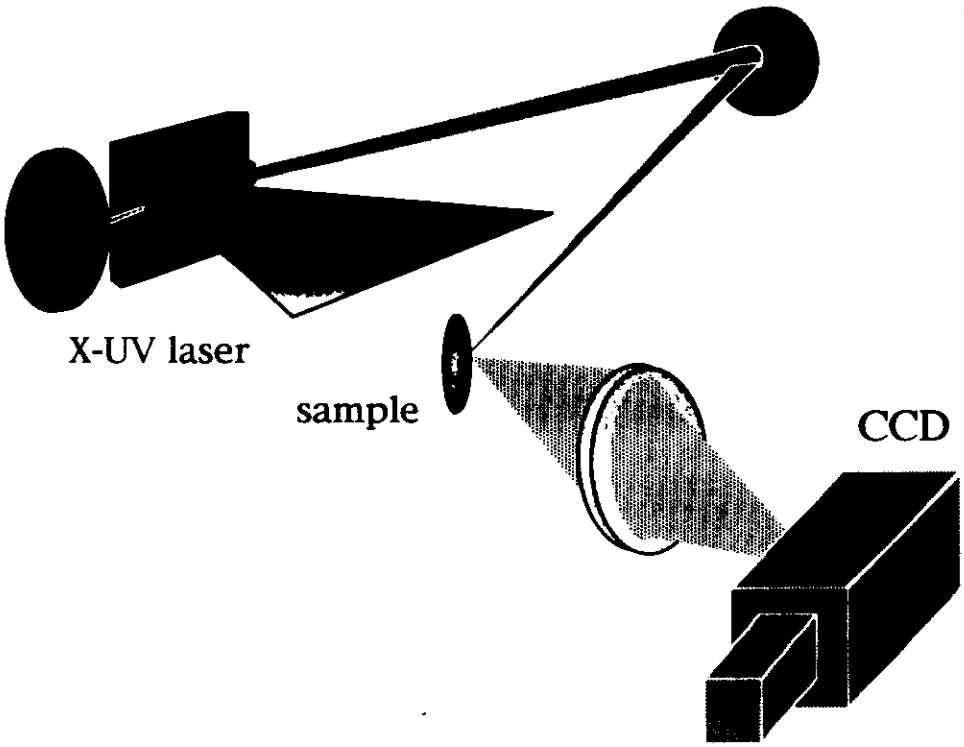

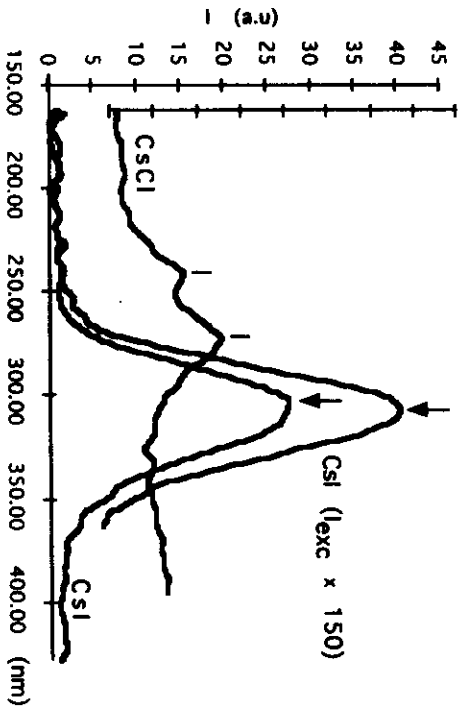

X-ray laser (21.2 nm) excited luminescence

LULI-LSAI

FUTURE X-RAY LASER STATION

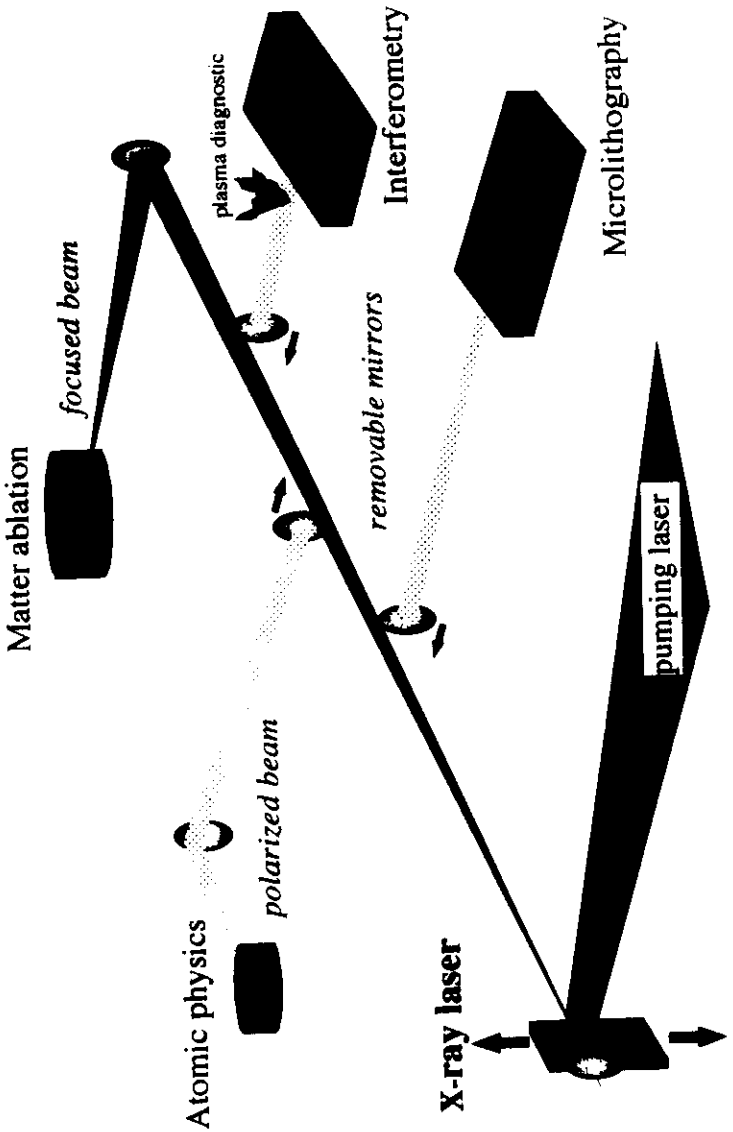

REFERENCES

1. J. Trebes et.al., Science **238**, 517 (1987).
   Y. Nato et.al, SPIE vol 2012, pp 12, (1993)

2. D.S. Di Cicco et.al, p277 in OSA Procceedings on Short Wavelength Coherent Radiation and applications, Ed. R. Falcone adn J. Kirz, (1988).

3. C. Skinner et.al, J. of Microscopy, **159**, 51 (1989).

4. J. Trebes, pp21 in "Applications of x-ray lasers", Procc. of Workshop. Ed. R. London, D. Matthews, and S. Suckewer, (1992).

5. L.B. Da Silva, et.al, Phys.Rev.Lett 74, 3991, (1995).

6. A.S. Wan et.al, pp. 504 in "X-Ray lasers 1996", Int. Comp. Ser. No. 151, Ed. S. Svanberg and C.G. Wahlström.

7. R. Caube et.al, Phys. Rev. Lett. 74, 3816 (1995).

8. S. Sebban et.al, p528, in "X-Ray lasers 1996", Int. Comp. Ser. No. 151, Ed. S. Svanberg and C.G. Wahlström.

ACKNOWLEDGMENTS:

Dr. LUIZ.B.DA SILVA (LAWRENCE LIVERMORE LABORATORY, USA)
Prof. PIERRE JAEGLE (LULI LSAI, FRANCE)